A 3.1-4.8GHz IR-UWB All-Digital Pulse Generator in 0.13-um CMOS Technology for WBAN Systems

Yun Ho Choi

Analog, Digital and RF circuit design Major
School of Electrical and Computer Engineering
Graduate school of UNIST

2012

A 3.1-4.8GHz IR-UWB All-Digital Pulse Generator in 0.13-um CMOS Technology for WBAN Systems

Yun Ho Choi

Analog, Digital and RF Circuit design Major
School of Electrical and Computer Engineering
Graduate school of UNIST

A 3.1-4.8GHz IR-UWB All-Digital Pulse Generator in 0.13-um CMOS Technology for WBAN Systems

A thesis
submitted to the School of Electrical and Computer Engineering
and the Graduate School of UNIST
in partial fulfillment of the
requirements for the degree of
Master of Science

Yun Ho Choi

12.28. 2011
Approved by

Major Advisor
Franklin Bien

A 3.1-4.8GHz IR-UWB All-Digital Pulse Generator in 0.13-um CMOS Technology for WBAN Systems

Yun Ho Choi

This certifies that the thesis of Yun Ho Choi is approved.

12. 29. 2011

Thesis Supervisor: Franklin Bien

Youngmin Kim: Thesis Committee Member #1

Jingook Kim: Thesis Committee Member #2

Abstract

Impulse Radio Ultra-WideBand (IR-UWB) systems have drawn growing attention for wireless sensor networks such as Wireless Personal Area Network (WPAN) and Wireless Body Area Network (WBAN) systems ever since the Federal Communications Commission (FCC) released the spectrum between 3.1 and 10.6GHz for unlicensed use in 2002. The restriction on transmitted power spectral density in this band is equal to the noise emission limit of household digital electronics. This band is also shared with several existing service, therefore in-band interference is expected and presents a challenge to UWB system design.

UWB devices as secondary spectrum users must also detect and avoid (DAA) other licensed users from the cognitive radio's point of view. For the DAA requirement, it is more effective to deploy signal with variable center frequency and a minimum 10dB bandwidth of 500MHz than a signal covering the entire UWB spectrum range with fixed center frequency.

A key requirement of the applications using IR-UWB signal is ultra-low power consumption for longer battery life. Also, cost reduction is highly desirable. Recently, digital IR-UWB pulse generation is studied more than analog approach due to its lower power consumption.

An all-digital pulse generator in a standard 0.13-um CMOS technology for communication systems using Impulse Radio Ultra-WideBand (IR-UWB) signal is presented. A delay line-based architecture utilizing only static logic gates and leading lower power consumption for pulse generation is proposed in this thesis. By using of all-digital architecture, energy is consumed by CV^2 switching losses and sub-threshold leakage currents, without RF oscillator or analog bias currents. The center frequency and the fixed bandwidth of 500MHz of the output signal can be digitally controlled to cover three channels in low band of UWB spectrum. Delay based Binary Shift Keying (DB-BPSK) and Pulse Position Modulation (PPM) schemes are exploited at the same time to modulate the transmitted signals with further improvement in spectrum characteristics. The total energy consumption is 48pJ/pulse at 1.2V supply voltage, which is well suitable for WBAN systems.

Contents

List of Figures

List of Tables

Nomenclature

ADC Analog-to-Digital Converter.

ADO All-Digital Oscillaor.

AGC Automatic Gain Control.

BPSK Binary Phase Shift Keying.

BRF Predicted output voltage according to BRF and channel.

CMOS Complementary Metal Oxide Semiconductor.

DAA Detect And Avoid.

DB-BPSK Delay-Based Binary Shift Keying.

DS-UWB Direct-Sequence Ultra-WideBand

EIRP Equivalent Isotropically Radiated Power.

FCC Federal Communications Commission.

ISM Industrial Scientific Medical.

IR-UWB Impulse-Radio Ultra-WideBand.

LNA Low Noise Amplifier.

LO Local Oscillator.

MB-OFDM Multi-Band Orthogonal Frequency Division Multiplexing.

MEMS Micro-Electro Mechanical System.

MICS Medical Implant Communication Service.

NMOS N-channel Metal Oxide Semiconductor.

OOK On-Off Keying.

PA Power Amplifier.

PAM Pulse Amplitude Modulation.

PDK Process Design Kit.

PMOS P-channel Metal Oxide Semiconductor.

PPM Pulse Position Modulation.

PSD Power Spectral Density.

RFID Radio Frequency IDentification.

UWB Ultra-WideBand.

VGA Variable Gain Amplifier.

WAN Wide Area Network.

WBAN Wireless Body Area Network.

WLAN Wireless Local Area Network.

WMAN Wireless Metropolitan Area Network.

WPAN Wireless Personal Area Network.

WSAN Wireless Sensor and Actuator Network.

Chapter I

Introduction

The successful realization of a Wireless Body Area Network (WBAN) requires innovative solutions to meet the power consumption budget of the autonomous sensor nodes. The radio interface is a major challenge, since its power dissipation must be reduced below 1mW/Mbps. The emerging Ultra-WideBand (UWB) technology shows strong advantages in reaching this target. First, the very little hardware complexity of an UWB transmitter offers the potential for low-cost and highly integrated solutions. Second, in a pulse-based UWB scheme, the transmitter can be duty-cycled at the pulse rate, thereby reducing the baseband power consumption.

This chapter demonstrates each technology, WBAN and UWB, and why RF systems using UWB signal are utilized for WBAN applications. As a result, the contribution points for WBAN systems in this thesis are stated.

1.1. WBAN Technology

With the rapid advancements of wireless communication and semiconductor technologies the area of sensor network has grown significantly supporting a range of applications including medical and healthcare systems. A Wireless Body Area Network (WBAN) is a special purpose sensor network designed to operate autonomously to connect various medical sensors and appliances, located inside and outside of a human body. Introduction of a WBAN for medical monitoring and other applications will offer flexibilities and cost saving options to both health care professionals and patients. A WBAN system can offer two significant advantages compared to current electronic patient monitoring system. The first advantage is the mobility of patients due to use of portable monitoring devices. Second advantage is the location independent monitoring facility. A WBAN node being an autonomous device can search and find a suitable communication network to transmit data to a remote database server for storage. It is also possible that a WBAN will connect itself to the internet to transmit data in a non-invasive manner. There are several advantages summarized by using WBANs which include:

- Flexibility: Non-invasive sensors can be used to automatically monitor physiological readings, which can be forwarded to nearby devices, such as a cell phone, a wrist watch, a headset, a PDA a laptop, or a robot, based on the application needs.

- -Effectiveness and efficiency: The signals that body sensors provide can be effectively processed to obtain reliable and accurate physiological estimations. In addition, their ultra-low-

Classification	Specification
Transmission distance	Maximum distance 3m or 5m
Data transmission throughput	1kbps ~ 10Mbps (100Mbps is optional)
Band for use	MICS, UWB, ISM
The maximum number of sensors and devices per a network	100
Duty Cycle	0.1 ~ 100%
Power management	1mW/Mbps at 1m

Table 1-1: Technical requirements of WBAN system.

power consumption makes their batteries long-lasting due to their ultra-low power consumption.

- Cost-effective: With the increasing demand of body sensors in the consumer electronics market, more sensors will be mass-produced at a relatively low cost, especially in gaming and medical environment.

And technical requirements of WBAN are described in Table. 1-1. Big differences of WBAN, from other existing systems, is to consumes ultra-low power and to give a variation to data throughput from low rate to high rate.

1.1.1. WBAN Communication Architecture

The development and research in the domain of WBANs is only at an early stage. As a consequence, the terminology is not always clearly defined. In literature, protocols developed for WBANs can span from communication between the sensors on the body to communication from a body node to a data center connected to the internet. [1] gives us clear understanding with the following definitions: Intra-body communication and Extra-body communication. An example is shown on Figure 1-1.

In Figure 1-2, a WBAN is compared with other types of wireless networks, such as Wireless Personal Area Network (WPAN), Wireless Local Area Network (WLAN), Wireless Metropolitan Area Network (WMAN) and Wide Area Network (WAN). A WBAN is operated close to the human body and its communication range will be restricted to a few meters, with typical values around 1-3meters. While a WBAN is devoted to interconnection of one person's wearable devices, a WPAN is a network in the environment around the person. The communication range can reach up to 10m for high data ra-

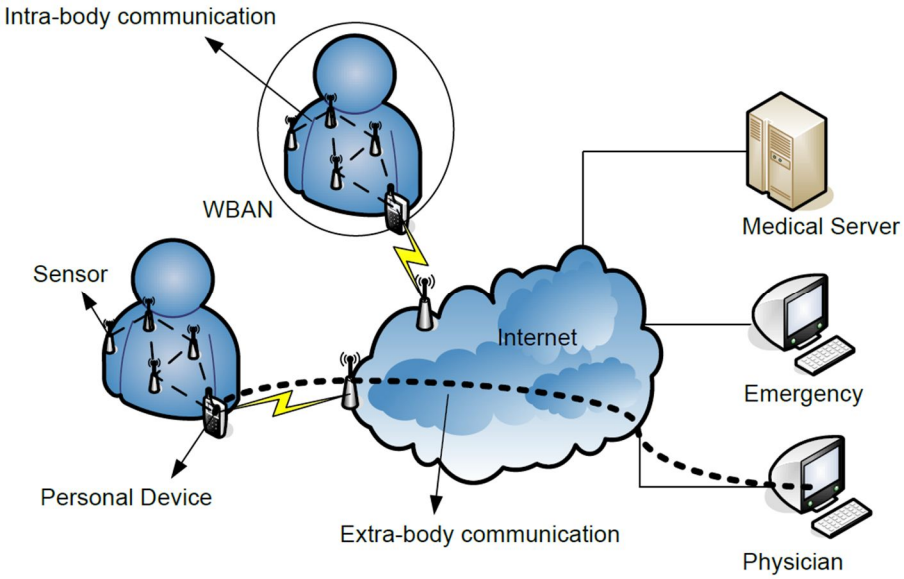

Figure 1-1: Example of intra-body and extra-body communication in a WBAN.

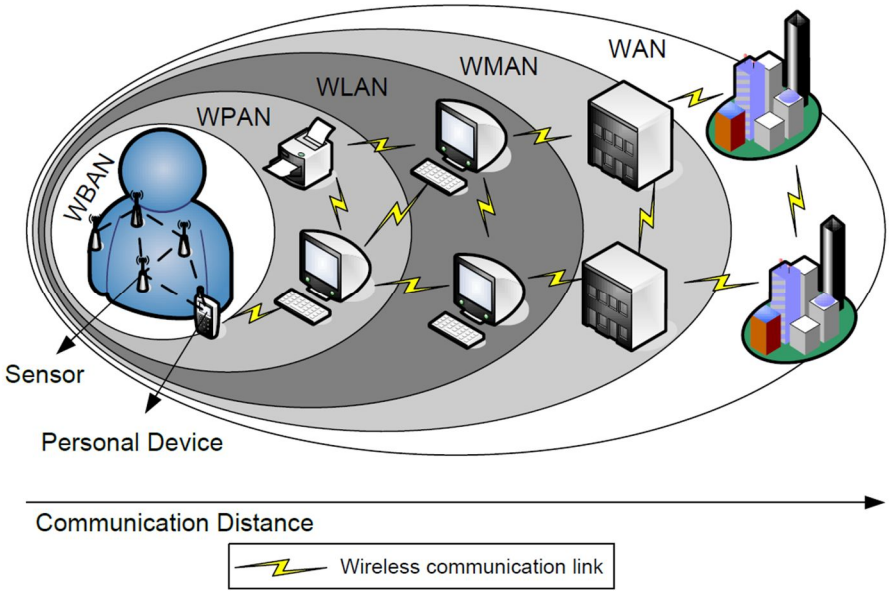

Figure 1-2: Positioning of a Wireless Body Area Network in the realm of wireless networks.

te applications and up to several dozens of meters for low data rate applications. A WLAN has a typical communication range up to hundreds of meters. Each type of network has its typical enabling technology, defined by the IEEE. A WPAN uses IEEE 802.15.1 (Bluetooth) or IEEE 802.15.14 (ZigBee), A WLAN uses IEEE 802.11 (WiFi) and a WMAN IEEE 802.16 (WiMax). The communication in a WAN can be established via satellite links.

In several papers, Wireless Body Area Networks are considered as a special type of a Wireless Sensor Network or a Wireless Sensor and Actuator Network (WSAN) with its own requirements. Ho-

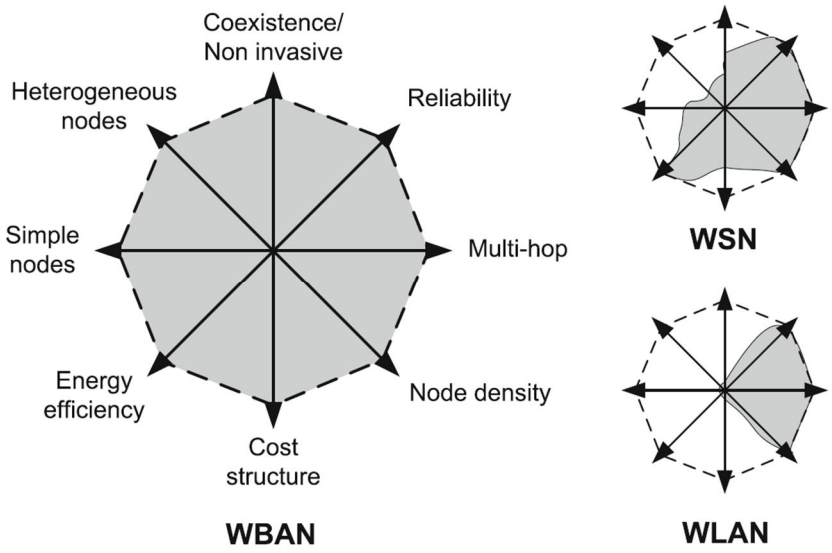

Figure 1-3: Characteristics of a WBAN compared with WSN and WLAN.

wever, traditional sensor networks do not tackle the specific challenges associated with human body monitoring. The human body consists of a complicated internal environment that responds to and interacts with its external surroundings, but is in a way separate and self-contained. The human body environment not only has a smaller scale, but also requires a different challenge than those faced by WSNs. The monitoring of medical data results in an increased demand for reliability. The ease of use of sensors placed on the body leads to a small form factor that includes the battery and antenna part, resulting in a higher need for energy efficiency. Sensor nodes can move with regard to each other, for example a sensor node placed on the wrist moves in relation to a sensor node attached to the hip. This requires mobility support. In brief, although challenges faced by WBANs are in many ways siliar to WSNs, there are intrinsic differences between the two, requiring special attention. A schematic overview of the challenges in a WBAN and a comparison with WSNs and WLANs is given in Fig. 1-3.

1.1.2. Hardware and Devices

A body sensor node mainly consists of two parts: the physiological signal sensor(s) and the radio platform, to which multiple body sensors can be connected. The general functionality of body sensors is to collect analog signals that correspond to human's physiological activities or body actions. Such an analog signal can be acquired by the corresponding radio-equipped board in a wired fashion, where the analog signal is digitized. Finally, the digital signal is forwarded by the radio transceiver.

As data sources of the WBAN system, body sensors are used for collecting the vital signals of a user of patient. Based on these body signals, an accurate diagnosis can be obtained to give the patient-

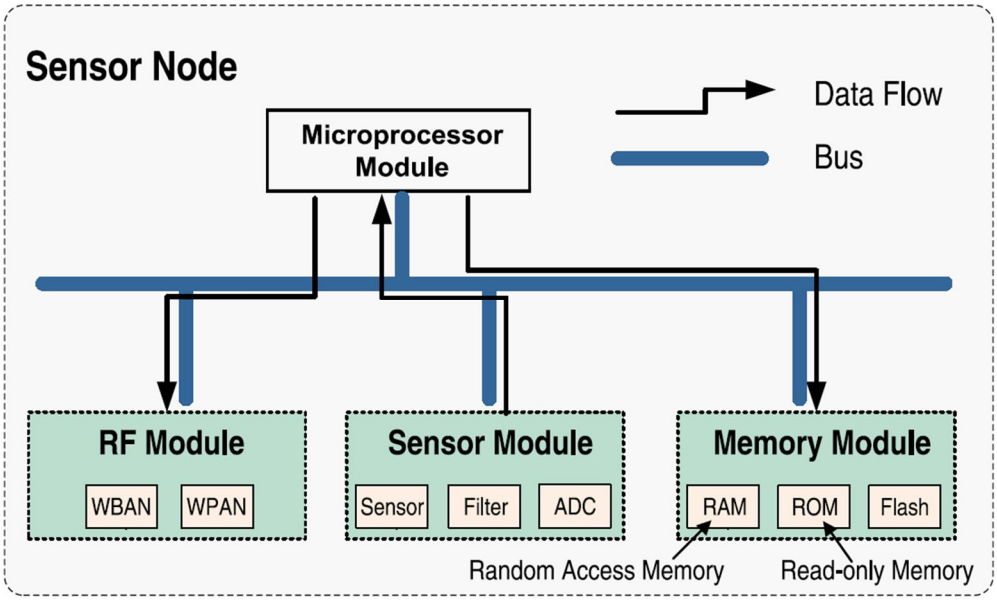

Figure 1-4: Typical modules on a sensor node.

correct and timely treatments. Traditionally, measurements via body sensors involve human intervention by medical staff. With the continuous advances in circuit design, signal processing, and Micro-Electro Mechanical Systems (MEMS), body sensory data can be collected in a non-invasive fashion. Body sensor devices are also becoming smaller and wearable, which make WBANs more likely to be deployed in a highly dynamic and pervasive environment, compared to previous medical systems. As a result, medical facilities can be significantly reduced, while improving the quality of medical services and healthcare.

Fig. 1-4 shows a typical sensor node with sensor, radio and memory modules [2]. The sensor module consists of a sensor, a filter and an analog-to-digital converter (ADC). The sensor converts some form of energy to analog electric signals, which are bandpass-filtered and digitized by the ADC for further processing. The challenges of the wireless technology (RF module) can be, for example, interference by and to the other devices, battery life and reliability of transmissions. In the hospital environment especially, it is important that any device is not causing harmful radiation to humans or interference to other electronic devices. The reliability of transmissions is extremely important since wrong data can cause wrong conclusions which in the case of physiological parameters can cause even life threatening treatments.

There exist several possible technologies for WBAN, i.e., Bluetooth, ZigBee and Ultra-WideBand (UWB), each with advantages and disadvantages. ZigBee offers low power consumption but with restricted data rate. Bluetooth is mature and cheap technology with fairly high power consumption [4]. However, the stringent energy consumption requirement of the future-WBAN cannot be met by toda-

Standard	Bluetooth	ZigBee	UWB	
IEEE Spec.	802.15.1	802.15.4	802.15.3a	802.15.4a
Freq. band	2.4GHz	868/915MHz; 2.4GHz	3.1-10.6GHz	3.1-10.6GHz
Max signal rate	1Mbps	250Kbps	110Mbps, 480Mbps	1Mbps
Nominal range	10m	10-100m	10m, 2m	30m
Tx power	0-10dBm	0-20dBm	-41.3dBm	-41.3dBm
# of RF channels	79	1/10; 16	1-15	1-15
Channel bandwidth	1MHz	0.3/0.6MHz; 2MHz	500MHz – 7.5GHz	500MHz – 7.5GHz

Table 1-2: Comparison of the Bluetooth, ZigBee and UWB.

y's low-power short-range radios such as Bluetooth and ZigBee. Recently, FCC opened a 3-10GHz band in the US for use by low-power ultra wideband (UWB) transceivers provided within a range of 3.1-10.6GHz, with minimum bandwidth of 500MHz, and has power spectral density below -41.3dBm/MHz. UWB is a technology in WPAN (IEEE 802.15.3a & IEEE 802.15.4a) in which very high data rates (480Mb/s) can be achieved at short distances of just a few meters. This can be used for audio/video streaming applications. It has two proposals: one is a multi-band Orthogonal Frequency Division Multiplexing (MB-OFDM) supported by WiMedia Alliance and the other is Direct Sequence UWB (DS-UWB) supported by UWB forum. In pulse-based UWB, the transmitter only needs to operate during pulse transmission, which reduces baseline power consumption. In UWB communication, most of the complexity is in the receiver to realize ultra-low power. The minimum complexity of the UWB transmitter offers the potential for low-cost and highly integrated solution (eg, endoscopy with a micro-camera). To further reduce power consumption, a multi-hop approach is promising where a sensor does not transmit its data directly to a master node but forwards to several intermediate nodes (transmission from a node on the back to a node on the chest). Most of the transmitters are switched off between pulses [5]. In UWB, diffraction is the main propagation around the human body and surface waves and reflections are negligible. A UWB-RAKE receiver with one or two fingers is sufficient to collect 50-80% of maximum energy for links with a distance of 15 cm, independently upon its placement on the body.

Recently developed short-range UWB technology could be used for WBAN application due to its low transmit power shown in Table 1-2. The implanted wireless nodes in a patient's body should form a WBAN so that one or more implanted devices inserted in the bodies of several patients in a hospital environment can be controlled with minimum complexity. The system uses a Radio Frequency (RF) transceiver designed to be used for in-body communication system. The devices use the new medical band Medical Implant Communication Service (MICS) together with 433 MHz ISM band to form a

medical sensor network of implant devices. The MICS band has a low emission power of 25 uW, comparable to that of UWB [6]. The UWB is a narrow pulse-based transmission system whose spectrum is spread across a wide range of frequencies. UWB transmission power is lower than ZigBee, Bluetooth, which is less likely to affect human tissue and causes interference to other medical equipment. It can transmit at higher data rate, which is suitable for real-time continuous monitoring of a number of physiological signals.

1.2. UWB Technology

As explained in previous section, Ultra-WideBand (UWB), approved by Federal Communications Commission (FCC) in February of 2002 [7]-[8], is a radio technology that can be at very low energy levels for short-range high-speed communications using a large bandwidth(>500MHz). UWB technology has been proposed for WBAN by the IEEE 802.15.6 Task Group (TG). The main application field of WBAN centers on the human body, a spectrum sensitive environment which requires low radiation. The sensors should be small. They are expected to be wearable or even implantable in human bodies; therefore, they can only support batteries with limited capacity. All of these factors make UWB an ideal technology for WBAN applications due to its low radiation power, high power efficiency, and most importantly, its high data rate in a small transmission range.

1.2.1. UWB Signal Characteristic

UWB communication systems are commonly defined as systems with large absolute and/or large relative bandwidth. Such a large bandwidth offers specific advantages with respect to signal robustness, information transfer speed, and/or implementation simplicity, but leads also to fundamental differences from conventional, narrowband, systems (in Fig. 1-5). Though the history of UWB reaches back to the 19^{th} century (e.g., Hertz's experiments using spark-gap transmitters), it was only in the last decade that a confluence of technological and political/economic circumstances enabled widespread commercial use of UWB systems. Consequently, research in UWB has grown dramatically recently.

Part 15 of FCC rules provides the following definitions for UWB operation (application system definitions are omitted):

- UWB bandwidth: For the purpose of this subpart, the UWB bandwidth is the frequency band bounded by the points that are 10dB below the highest radiated emission, as based on the complete transmission system including the antenna. The upper boundary is designated f_H and the lower boundary is designated f_L. The frequency at which the highest radiated emission occurs is designated f_M.

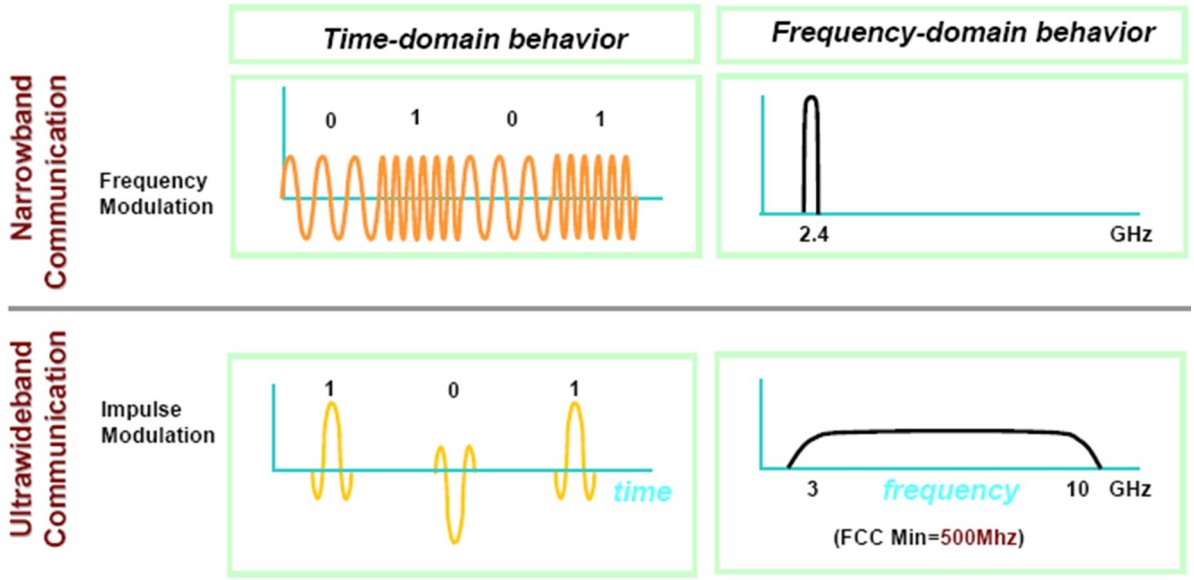

Figure 1-5: Fundamental differences between UWB and narrowband.

- Center frequency: The center frequency, f_C, equals $(f_H+f_L)/2$.
- Fractional bandwidth: The fractional bandwidth equals $2(f_H-f_L)/(f_H+f_L)$.
- UWB transmitter: An intentional radiator that, at any point in time, has a fractional bandwidth equal to or greater than 0.20 or has a UWB bandwidth equal to or greater than 500MHz, regardless of the fractional bandwidth.
- EIRP: Equivalent isotropically radiated power, i.e., the product of the power supplied to the antenna and the antenna gain in a given direction relative to an isotropic antenna. The EIRP, in terms of dBm, can be converted to field strength, in dBuV/m at 3 meters, by adding 95.2. With regard to this part of the rules, EIRP refers to the highest signal strength measured in any direction and at any frequency from the UWB device. As a result, its value is -41.3dBm per 1MHz.

The interest in UWB systems stems mainly from the fact that they can be used as an overlay to existing systems. In other words, they do not require new spectrum, but can be operated in parallel to existing legacy systems. This can be understood from the simple picture in Fig. 1-6: the transmit power of any system can be (approximately) expressed as the product of power spectral density (PSD) and bandwidth. A large (absolute) bandwidth thus enables a system with reasonable transmit power to exhibit an extremely low power spectral density. A victim legacy (narrowband) receiver will only see the noise power within its own system bandwidth, i.e., a small part of the total transmit power. This implies that the interference to legacy (narrowband) systems is very small.

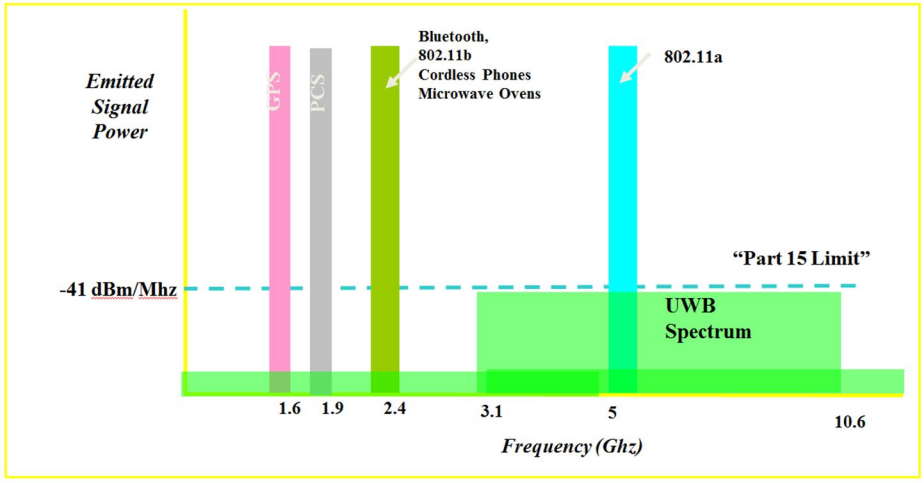

Figure 1-6: Fundamental differences between UWB and narrowband.

The large absolute bandwidth allows a transmission of extremely high data rates (>100Mbps), though the transmission can be achieved only over relatively short distance (<10m) because only very low power is available for each bit. Alternatively, low-data-rate communication (e.g., <1Mbps) is possible over much larger distances by exploiting the large spreading factor (ratio between used bandwidth and data rate).

A large relative bandwidth also offers advantages to UWB systems, in particular a greater robustness of the signals. Intuitively, the different frequency components of the signal "see" different propagation conditions. Thus, there is a high probability that at least some of them can penetrate obstacles or otherwise make their way from transmitter to receiver. Consequently, the signal is more robust to shadowing effects.

1.2.2. UWB Applications

UWB communication is being considered for a wide range of applications. UWB chipsets have been demonstrated in short range, high data rate applications including streaming video from a DVD player to an in-home TV, or to headrest-mounted LCD displays in a vehicle. Wireless USB has also been demonstrated over UWB, and the first wireless USB product appeared in 2006. UWB offers the potential for precise locationing capabilities, therefore it is also being used for RFID tagging and low data rate, long range communication. One of the largest applications in this space has been for asset and patient tagging in hospitals.

1.2.2.1. High Data Rate Applications

The IEEE created the 802.15.3a TG in 2002 to investigate using UWB as a physical layer for high data rate, short range wireless personal area networks (WPAN). This task group solicited proposals for

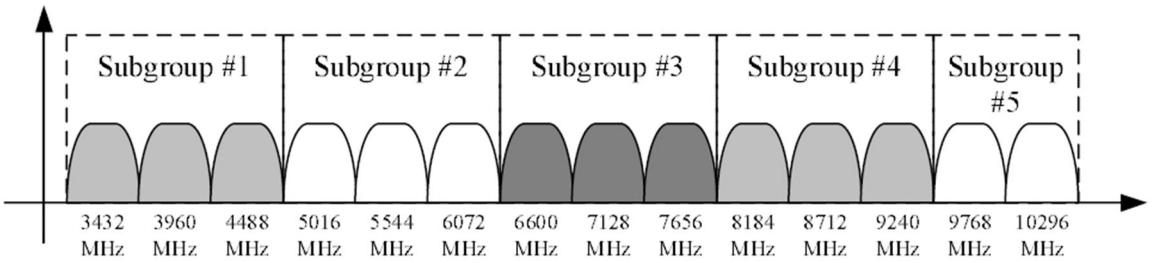

Figure 1-7: Band plan for the WiMedia Alliance OFDM based proposal for WPAN.

a new WPAN standard, requiring that all proposals submitted to the committee to meet certain specifications. The minimum specifications were a data rate of 100Mbps at 10m and 200Mbps at 4m with a maximum power consumption of 100mW and 250mW, respectively, and a maximum uncoded bit error rate (BER) of 10^{-9}. Additionally, data rate greater than 480Mbps is desirable, even if it operates at reduced ranges. Four piconets in close proximity were required to simultaneously operate at these data rates. These specifications are sufficient for most WPAN applications.

The 802.15.3a TG had narrowed the proposals for a WPAN standard down to two by 2005: one OFDM based, and one pulse based. The TG was disbanded in 2006 when an agreement couldn't be reached on which proposal should become the standard.

- OFDM proposal: Proposed by the MultiBand OFDM Alliance (MBOA) [8], and later adopted by the WiMedia Alliance, this technical approach uses an OFDM standard that essentially expands on other current OFDM physical layers, such as 802.11g. The supported data rates range from 53.3Mbps to 480Mbps. The transmitted signal is synthesized with a high speed DAC, and can therefore be very spectrally efficient compared to pulse-based transmitters. OFDM modulation is inherently robust against channel multi-path, as well as gain, phase variations in the transceiver. This proposal divides the UWB band into 14 channels, spaced 528MHz apart, as show in Fig. 1-7. The channels are grouped into subgroups of two or three channels, and frequency hopping is implemented within each subgroup.

  As the OFDM transmitter hops among three bands in a band group, it transmits a power level that is three the maximum FCC limit. Therefore, at any given time, the transmitter uses one third the bandwidth and three times the power spectral density. As the transmitter rapidly hops among the three channels in the subgroup, the emissions average out to the FCC limit in any given channel. The higher transmit power can pose an increased risk to victim receivers, however a waiver was granted by the FCC specifically for this approach. A drawback to this frequency hopping scheme is the rate at which hops are made must be less than 10ns with a maximum hop distance of 1056MHz. This is to be accomplished with a PLL, therefore multipl-

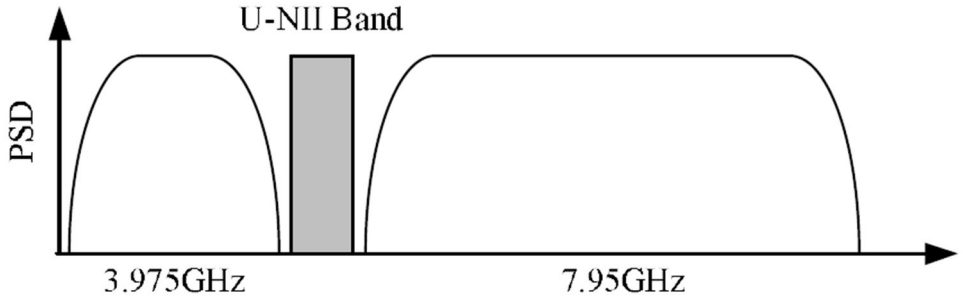

Figure 1-8: Band plan for the DS-UWB pulse based proposal for WPAN.

e oscillators are required with a either a multiplexer to select the LO, or replicated hardware in the RF front-end for each channel.

- DS-UWB proposal: The alternate proposal submitted to the 802.15.3a TG is direct sequence UWB (DS-UWB) architecture from the UWB Forum [9]. This architecture is pulse based, using BPSK modulation or an optional bi-orthogonal keying (BOK) mode. BOK modulation uses a set of orthogonal codes for direct sequence spreading, increasing the data rate by selecting a code based on the transmitted data. The signal is transmitted in two general bands. One from 3.1-4.85GHz and one from 6.2-9.7GHz as shown in Fig. 1-8. The actual center frequency depends on the piconet channel being used, and the channels are offset by 39MHz. The piconets are therefore designed with significant overlap, using baseband signal processing to resolve the channels. The supported data rates range from 28Mbps to 1320Mbps.

  One advantage of this architecture is many components of the baseband processor may be made scalable, such as the number of fingers in the rake receiver, the time duration of the equalizer, or the datapath bit widths. This scaling is attractive for energy efficiency, because the power consumption can scale gracefully with performance, depending on the signal SNR and multipath. The ability to scale the hardware sets the DS-UWB approach apart from OFDM systems. OFDM architectures do not scale as well and have hard limits on the minimum processing required for arbitrarily high SNR.

1.2.2.2. Low Data Rate, Tagging Applications

Another application well suited for UWB is radio frequency identification (RFID) tags. In September 2004, Parco Wireless installed a network of RFID tags using UWB for communication and locationing to track patients, staff, and equipment in a hospital. The tags relay battery status, tag tampering information, and status of the medical device to which they are attached using UWB technology [10]. The advantages of using UWB for this application are the startup time for the tag radios, and the positions of the tags can be tracked with sub-foot precision. The required data rate in t-

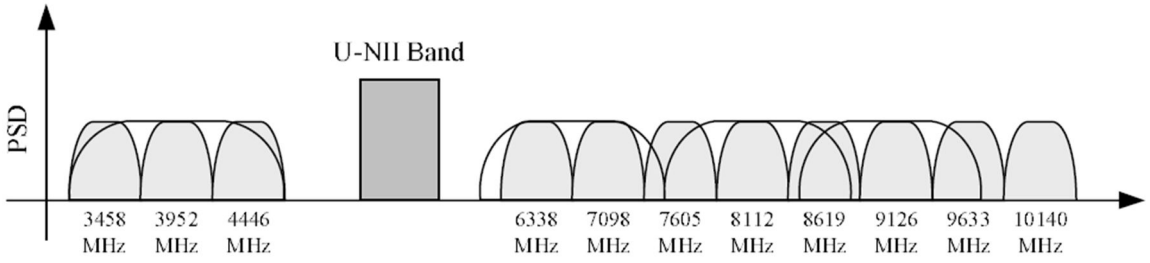

Figure 1-9: Band plan for the IEEE 802.15.4a for WPAN standard.

his application is less than 100bps, but data rates for RFID tags in general could be much lower. In this regime when buffering data is not practical, radio startup time dominates the energy consumption in the network. UWB circuits have transient responses on the order of 100ps, and often do not require a local oscillator and phase-locked loop to startup and settle. Therefore, they may be started up in a very short amount of time, reducing the total energy consumed in the network.

The IEEE has recently completed a standard, titled 802.15.4a, for short range, low data rate communication and ranging in a wireless personal area network (WPAN) [11]. The standard utilizes the 2.4GHz ISM band, sub-GHz UWB band, and 3.1GHz UWB band. The 3.1-10.6GHz band has been subbanded into the frequency plan shown in Fig. 1-9. The data rates supported range from 100kbps to 27Mbps, using pulse position modulation (PPM), or a combination of PPM and BPSK. This standard is extremely flexible, supporting several mandatory and optional modes to accommodate a range of radio architectures and applications. Finally, now IEEE 802.15.6 TG decides WBAN standards adopting many of IEEE 802.15.4a standards. And large amount of research activities are performed even though the WBAN standards have not been defined yet.

1.3. Thesis Contribution

This thesis focuses on the aspects of pulse generation for UWB transceivers which can be easily applied to WBAN system.

- All-Digital Pulse Generation: The available bandwidth in the UWB band far exceeds what is required for low data rate applications. UWB transceivers may capitalize on this fact by relaxing the specifications on frequency precision in order to reduce the energy/bit of the system. This approach has been applied to develop an all-digital UWB transmitter architecture that supports programmable pulse widths and center frequencies, without requiring an RF local oscillator. The transmitter has been demonstrated in a fabricated test chip in 0.13-um CMOS process. This transmitter is designed using only full-swing static CMOS circuits, and no analog biases are required.

- Delay-Based BPSK Modulation: For some forms of UWB modulation, the spectrum produced will contain tones even when modulated by purely random data. Spectrum scrambling is therefore required, and the most common technique used combines BPSK scrambling with other forms of UWB modulation to eliminate all tones. BPSK is costly to implement in all-digital architecture. A spectrum scrambling technique is proposed that is suitable for digital transmitter architectures, and produces the same scrambling effect as BPSK in the main lobe of the spectrum. This technique is also suitable for replacing BPSK as the sole pulse modulation in a coherent transceiver.

Chapter II

Technical Challenges & Approaches

This chapter demonstrates the challenges of UWB pulse generation for WBAN systems, and the technical approaches to solve those issues are discussed. Finally, the requirements to implement UWB pulse generation are stated.

2.1. DAA Requirement

Cognitive radios have been advanced as a technology for the opportunistic use of underutilized spectrum wherein secondary devices sense the presence of the primary user and use the spectrum only if it is deemed empty. Spectral cognition of this form can also be used by regulators to facilitate the dynamic coexistence of different service types. An example of this is the operation of ultra-wideband devices in WiMAX bands: UWB devices must detect and avoid (DAA) WiMAX devices in certain regulatory domains [12] since the FCC released the spectrum between 3.1 and 10.6GHz for unlicensed use in 2002. And each country has different DAA regulations shown in Fig. 2-1 [13]. Most countries have DAA technology used in the low band of UWB spectrum.

To coexist with broadband wireless networks, a UWB "detect and avoid" implementation should answer the following requirements [14]:

- The UWB device should employ a narrowband signal detection function that allows it to detect active broadband networks in the 3.1-4.8GHz frequency range, serving indoor terminals.

- Before initiating a UWB network in the frequency range 3.1-4.8GHz, the UWB device should perform a narrowband signal existence test. This test should be performed for a minimum duration and reliably to ensure that there are no broadband networks operating in that frequency range.

- If the results of either the initial channel availability check or the in-service monitoring indicate the presence of a broadband networks serving indoor clients in any of the bands (e.g. Channel 1, 2, 3), the UWB emissions levels over those respective bands should be reduced to a lower level. Optionally, the UWB device may also transmit standardized messages to other compatible UWB devices indicating the identity of these frequency bands.

- During normal operation in the 3.1-4.8GHz frequency range, the UWB device should monitor the frequency band to ensure there are no operating broadband networks using the detection fu-

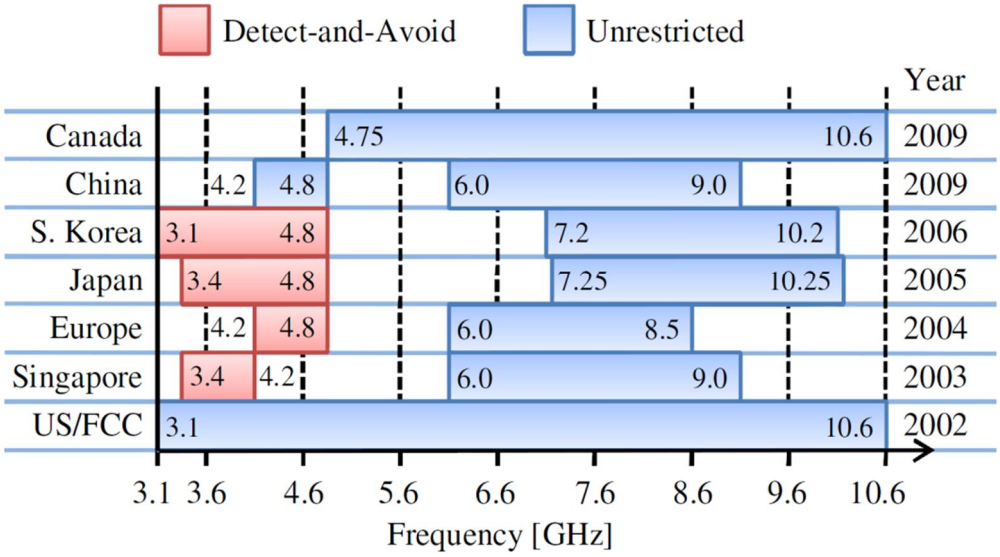

Figure 2-1: DAA plan for each country.

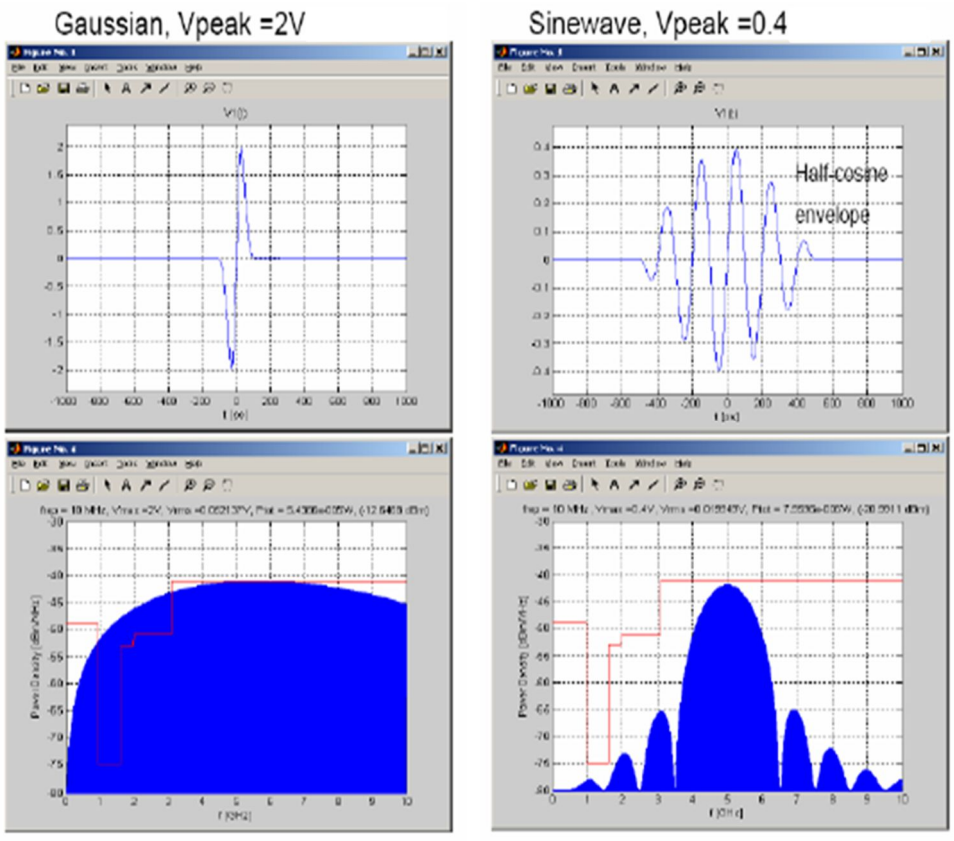

Figure 2-2: UWB pulses: carrier-less pulse (the left), carrier-based pulse (the right).

nction. The UWB device may perform this monitoring function during periods when it is not transmitting UWB signals, and can continue using the available channels until the presence of a broadband network signal is detected.

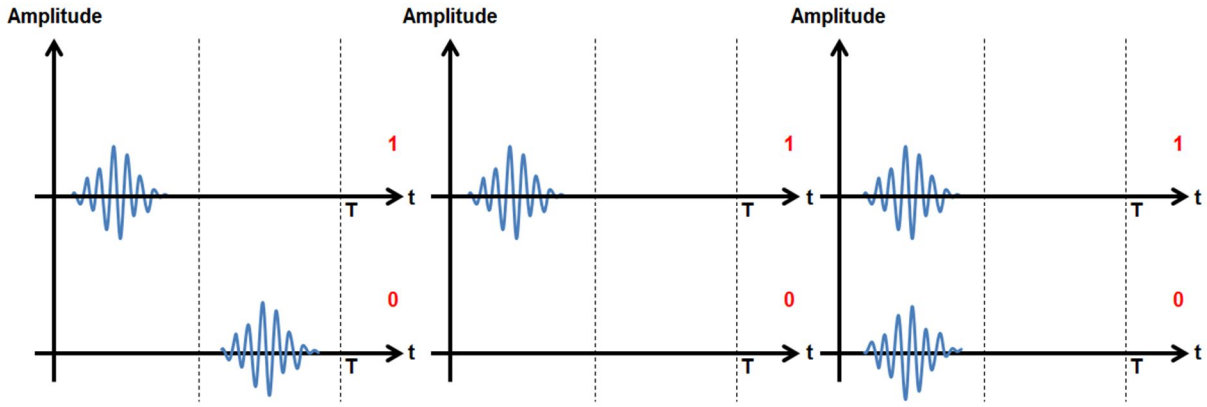

Figure 2-3: Modulation schemes: PPM, OOK and BPSK in regular sequence.

As a result, implementing frequency selectivity in signal transmission is the most important to transmit UWB signal according to DAA requirement. Reducing emission level is not effective way since the value of UWB radiation from transmitter is already low enough. Therefore it is the second operation for DAA requirement. Thus, carrier-based UWB pulse is recommended more frequently than carrier-less UWB pulse. The characteristic of each pulse is illustrated in Fig. 2-2 [15].

2.2. Modulation Schemes for UWB Communication

Information can be encoded in a UWB signal in a variety of methods. The most popular modulation schemes developed to date for UWB are pulse-position modulation (PPM) [16], pulse-amplitude modulation (PAM) [17], on-off keying (OOK) [18], and binary phase-shift keying (BPSK) [19], also called biphase. Other schemes are, of course, possible, but these modulation schemes have been selected by various groups to meet the different design parameters generated by different applications.

Of course, a UWB signal is not different from any other signal, and any other modulation scheme can be applied, including orthogonal or bi-orthogonal modulations. New systems are emerging today that utilize different modulation schemes made feasible by the UWB spectrum allocation that allows narrower bandwidth signals. Several companies have attempted to patent or have patented specific modulation schemes for UWB systems. As the community will realize that UWB follows the same fundamental principles of narrowband systems, and “a radio is a radio”, many of these systems will be found in the prior art and will be recognized [20] as well-known methods. This will have a positive consequence in the market, because it will allow companies to develop more competitive products without the worry of infringing any patents.

- PPM scheme: PPM is based on the principle of encoding information with two or more positions in time, referred to the nominal pulse position, as shown in Fig. 2-3. A pulse

transmitted at the nominal position represents a 0, and a pulse transmitted after the nominal position represents a 1. The picture shows a two-position modulation, where one bit is encoded in one impulse. Additional positions can be used to provide more bits per symbol. The time delay between positions is typically a fraction of a nanosecond, while the time between nominal positions is typically much longer to avoid interference between impulses.

- OOK scheme: OOK is based on the principle of encoding information with the amplitude of the impulses, as shown in Fig. 2-3. The picture shows a two-level modulation, respectively, for zero and lower amplitude, where one bit is encoded in one impulse. As with pulse position, more amplitude levels can be used to encode more than one bit per symbol.

- BPSK (Biphase) scheme: In biphase modulation, information is encoded with the polarity of the impulse, as shown in Fig 2-3. The polarity of the impulses is switched to encode a 0 or a 1. In this case, only one bit per impulse can be encoded because there are only two polarities available to choose from.

As a result, PPM and OOK modulation schemes give a possibility of implementation of non-coherent detection even though BPSK using coherent detection has the best spectrum characteristics among them (it is explained later). Thus, in order for lower complexity and lower power consumption, PPM is primarily used to modulate signal for data transmission.

2.3. Pulse Generation Architecture

This thesis focuses on the aspects of pulse generation for UWB transceivers; therefore, the scope of this section is narrowed to transmitters. Pulsed-UWB transmitter architecture is grouped into two categories defining how the pulse energy is generated in the 3.1-10.6GHz UWB band. One is analog technique using LO, Mixer and power amplifier (PA), and the other is digital method using a delay line.

2.3.1. Analog Approach

The first category includes transmitters that generate a pulse at baseband and up-converted it to a center frequency in the UWB band by mixing with a local oscillator (LO) [21]-[22]. The transmitter may not have an explicit mixer that performs the up-conversion mixing. This architecture is easiest identified by having a LO at the center frequency of the pulse. Fig. 2-4 shows the general case of analog pulse generation. The up-conversion architecture generally offers more diversity and control over the frequency spectrum, but at the cost of higher power since an LO must operate with static current source at the pulse center frequency, and power amplifier PA also consumes much power. This

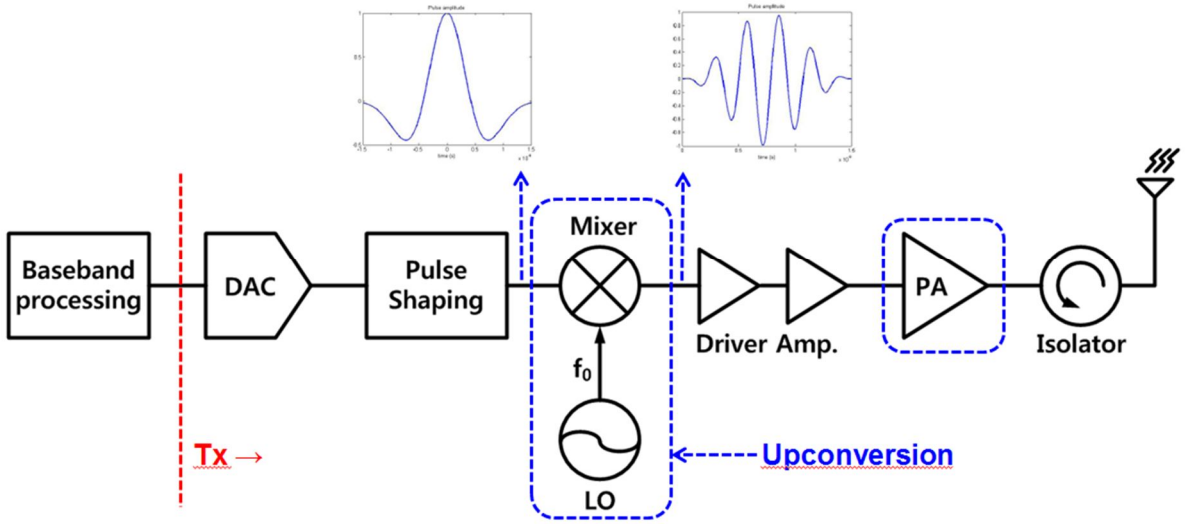

Figure 2-4: Typical analog type block diagram for UWB transmitter.

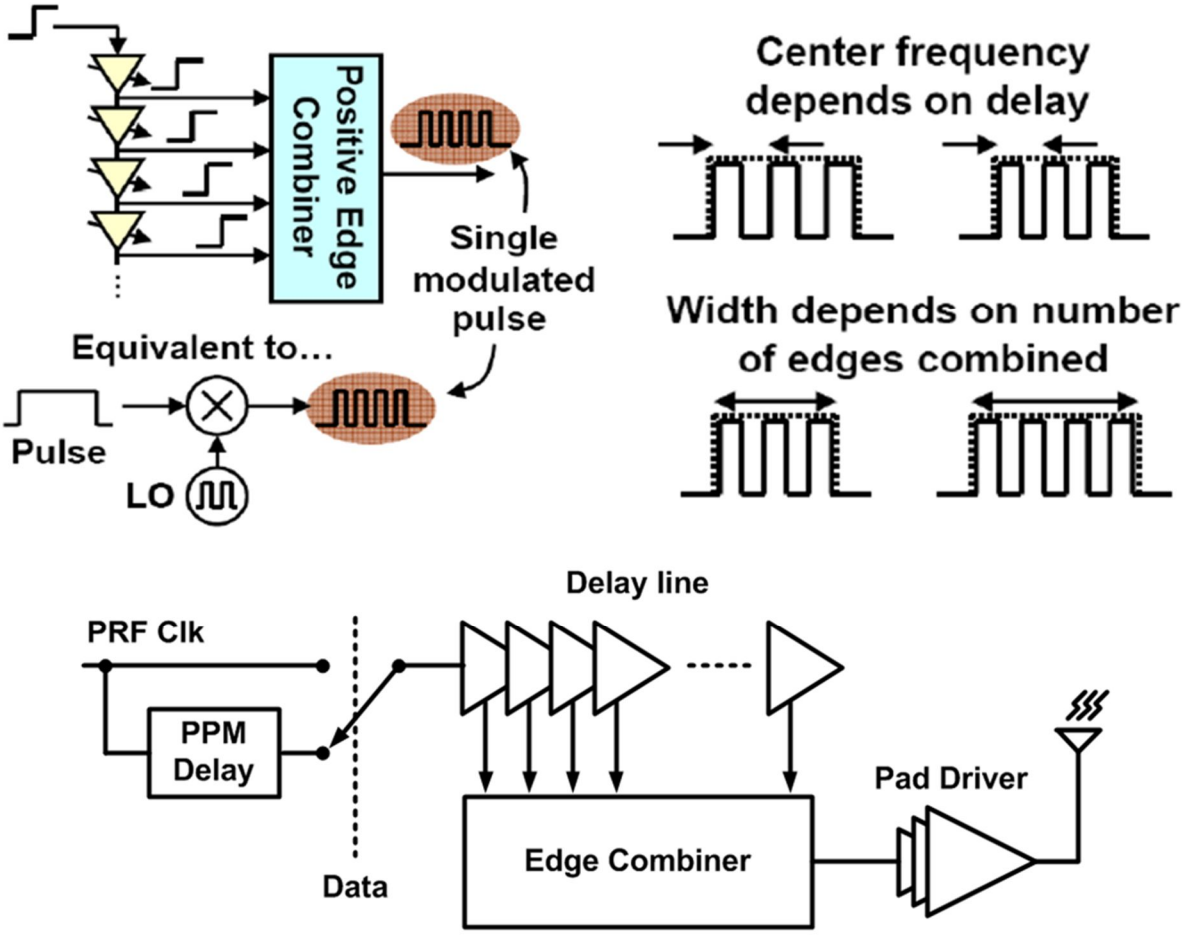

Figure 2-5: Digital concept for UWB transmitter.

architecture is usually found in high-data rate direct sequence communication system, where the pulse shape and center frequency must be well-defined.

	[28] Analog	[29] Analog	[30] Digital	[23] Digital
Technology	SiGe BiCMOS 0.18um	CMOS 0.18um	CMOS 0.18um	CMOS 90nm
Max. BRF	100MHz	31.2MHz	15.6MHz	16.7MHz
Frequency Range	3.1-10.6GHz	3-9GHz	3-5GHz	3.1-5GHz
Pulse Bandwidth	0.558GHz	~0.5GHz	~0.5GHz	~0.5GHz
Modulation	BPSK	PPM + BPSK	BPSK	PPM + DB-BPSK
Power consumption	31.3mW (Only LO, Mixer and PA)	23mW	1.45mW	0.789mW

Table 2-1: A summary of recently published pulsed-UWB transmitters.

2.3.2. Digital Approach

A transmitter that generates a pulse that directly falls in the UWB band without requiring frequency translation is described in Fig. 2-5 [23]. The pulse width for these types of transmitters is usually defined by delay elements that may be tunable or fixed, as opposed to oscillators. A baseband impulse may excite a filter that shapes the pulse [24]-[25], or the pulse may be directly synthesized at RF with no additional filtering required [26]-[27].

The energy consumption of this architecture is mainly contributed by the CV2, dynamic switching activities used for charging and discharging the capacitive components. The other source of energy consumption is the sub-threshold leakage. Because of using only full-swing static CMOS circuits, the architecture does not need to use PA, but to utilize driving circuit up to antenna.

2.3.3. Comparison between analog & digital type

A summary of recently published pulsed-UWB transmitters is in Table 2-1. It is interesting to note that the data rate of these transmitters varies from 15.6Mbps to 100Mbps, of course, sub-Mbps applications also exist. This goes to show the wide range of applications that UWB is being used for.

In the aspect of power consumption, data rate, which is equal to burst pulse repetition rate (BRF) that is constructed a single pulse or a bunched pulse to represent 1 or 0, directly relates to power dissipation. For impartial comparison, if we divide power consumption into max. BRF (this division -

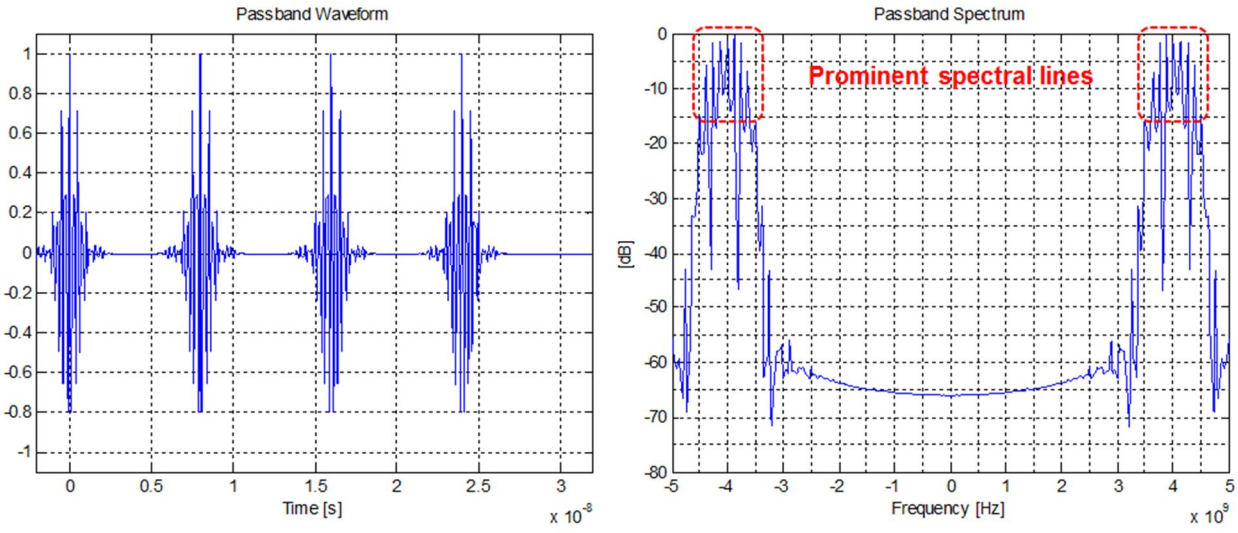

Figure 2-6: Periodic signal characteristic in time domain (the left) and in frequency domain (the right).

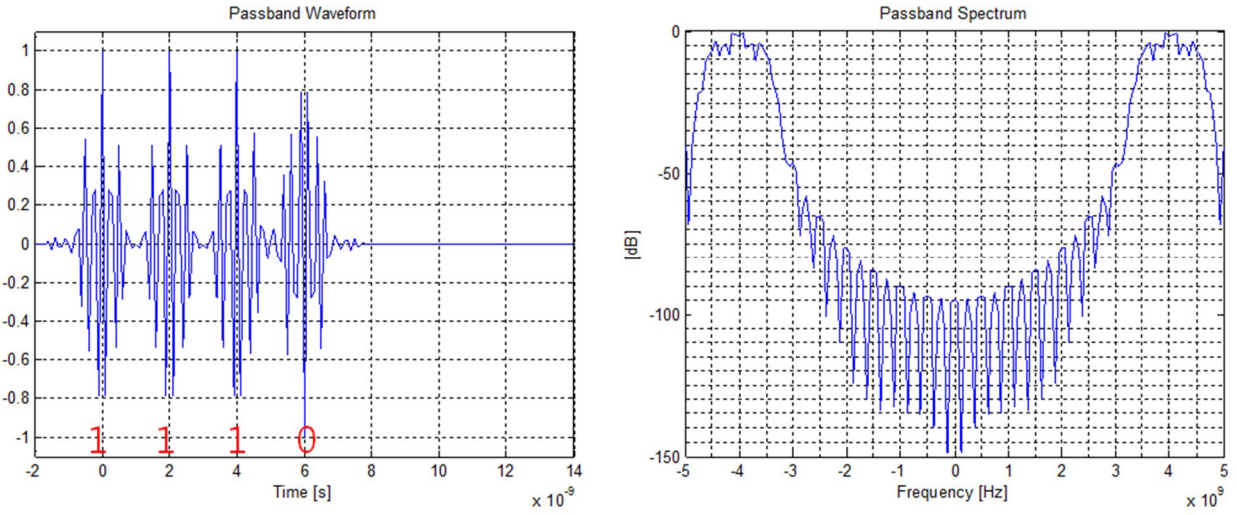

Figure 2-7: A pulse train modulated by BPSK in time domain (the letf) and in freq. domain (the right).

produces another expression, energy/pulse, which is explained in chapter Ⅲ), we can note that digital architecture consumes much less power when comparing to analog approach.

2.4. Spectral Line Problem

When a pulse train is periodic, its spectrum characteristic has a problem such as prominent spectral lines as shown in Fig. 2-6. This kind of phenomenon has output power reduced in order to meet FCC spectrum mask. PPM modulation scheme, which has been frequently used in IR-UWB systems, still includes spectral line problem. Giving random polarity to a pulse train is the way to reduce spectral line problem. BPSK has the best spectrum characteristic among binary modulations for UWB since its

polarity definitely breaks periodicity as illustrated in Fig. 2-7. However, BPSK has more complicated circuits. To overcome the drawback when using PPM modulation, DB-BPSK (delay based binary phase shift keying) phase scrambling needs to be additionally employed in the pulse generation stage even though PPM is mainly applied [23]. The implementation of DB-BPSK will be stated in chapter Ⅲ.

2.5. Summary on Design Targets & Technical Approaches

In this chapter, the direction of transmitter system design has been stated. Because DAA requirement, variable center frequency, or variable channel selection, has to be implemented. Digital architecture will be used due to its lower power consumption than analog approach that uses LO, mixer and PA. In order to reduce magnitude of spectral lines, PPM and DB-BPSK modulation schemes are exploited at the same time to modulate transmitted signals with further improvement in spectrum characteristics. Targeted specifications are as follows;

- Frequency range is from 3.1 up to 4.8GHz
- 10dB bandwidth is more than 500MHz
- Data rate: 1M – 100Mbps
- Power consumption is lower than 1mW/Mbps
- EIRP is lower than -41.3dBm/MHz

Chapter III

Transmitter System Design

This chapter demonstrates that an all-digital pulse generator as the most important block, directly related to transmitter system performance, in a standard 0.13-um CMOS technology for communication systems using impulse radio ultra-wideband (IR-UWB) signal. A delay line-based architecture utilizing only static logic gates and leading lower power consumption for pulse generation is proposed in this thesis. The center frequency and the fixed bandwidth of 500MHz of the output signal can be digitally controlled to cover three channels in low band of UWB spectrum. Delay based binary shift keying (DB-BPSK) is additionally employed to modulate signals with further improvement in spectrum characteristic, while pulse position modulation (PPM) is mainly applied to signal transmission.

3.1. Transmitter System Specification

System specification is directly related to the impulse signal used for communication system. In this thesis, the band group #2, the low band of UWB spectrum, including channel 1, 2 and 3, is utilized. The center frequency for each channel is 3.494GHz, 3.993GHz and 4.493GHz, respectively. However, actual implementation of center frequency of every channel is approximated 3.5GHz, 4GHz and 4.5GHz for easy calculation. Minimum 10dB bandwidth for each channel is approximately 500MHz.

The proposed pulse generation architecture is realized by digital circuits using a delay line and logic gates. Center frequency of transmitted signal immediately defines delay time. Pulse width, which is proportional to the number of fine pulses, relates channel bandwidth. A fine pulse is a pulse that has duration of delay time, and the time space between each fine pulse is also equal to delay time. As explained, the system parameters are well defined in Table 3-1 and in Fig. 3-1. Fig. 3-2 shows spectrum characteristic of an ideal single impulse signal by using MATLAB tool. Its center frequency is 4.5GHz targeted to channel 3. Absolute amplitude of the results in frequency domain is not important, but relative ratio between each value. 3dB bandwidth is close to 500MHz, and 10dB bandwidth is approximately 700MHz. From the simulation for ideal case, it is expected that the value of 10dB bandwidth is higher than 500MHz even after fabrication.

UWB transmits high amplitude pulses that only last for nanoseconds. The result is a high peak to average power. The question is: what is the transmitted power in the link budget calculation? In addition, some UWB systems detect single pulses rather than many pulses averaged over time. For th-

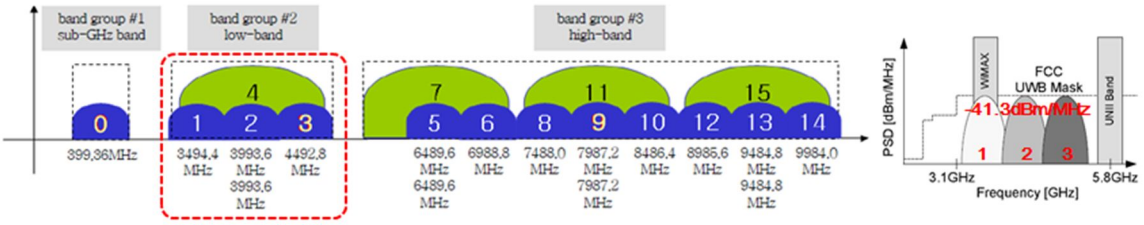

Figure 3-1: UWB band plan.

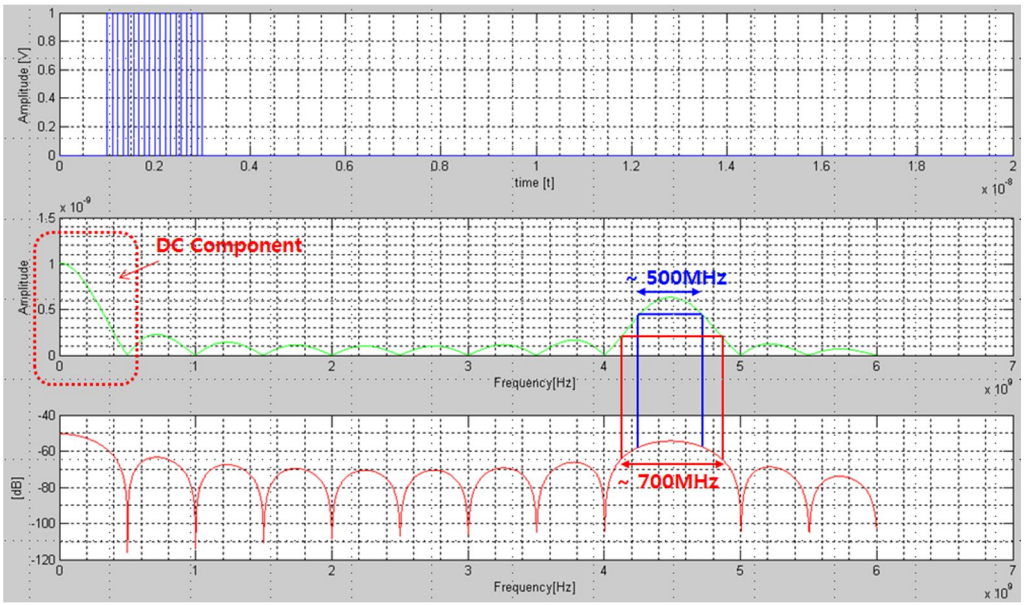

Figure 3-2: Spectrum characteristic of a single impulse for ideal case.

ese reasons, it make more sense to talk about transmitter energy per pulse rather than power in much the same way that energy per bit, which is equal to energy per pulse in this thesis and pulse here means burst pulse, is calculated in digital systems.

$$E_b = P \cdot T_b \quad (1)$$

P is the transmitted average power and T_b is the bit rate. This calculation assumes that each bit is represented by a squire pulse. UWB pulses are not square so it will be necessary to calculate the energy is the equivalent squire pulse [31]:

$$E_p = \int_{pulse-length} |x(t)|^2 \, dt \quad (2)$$

E_p is the energy in a single pulse and x(t) is the pulse. Since most UWB pulses have shapes that can be approximated by simple functions, it should be relatively easy to evaluate the expression in (2). The specific energy consumption in this thesis is described in Fig. 3-3.

Channel / Parameter	Channel 1	Channel 2	Channel 3
Center Frequency	3.494GHz	3.993GHz	4.493GHz
Frequency Range	3.245~3.746GHz	3.744~4.242GHz	4.243~4.742GHz
Channel Bandwidth	499.2MHz	499.2MHz	499.2MHz
Delay time	143.102psec	125.219psec	111.284psec
# of fine pulses	8	9	10
Pulse width	2.147nsec	2.129nsec	2.114nsec

Table 3-1: System specifications.

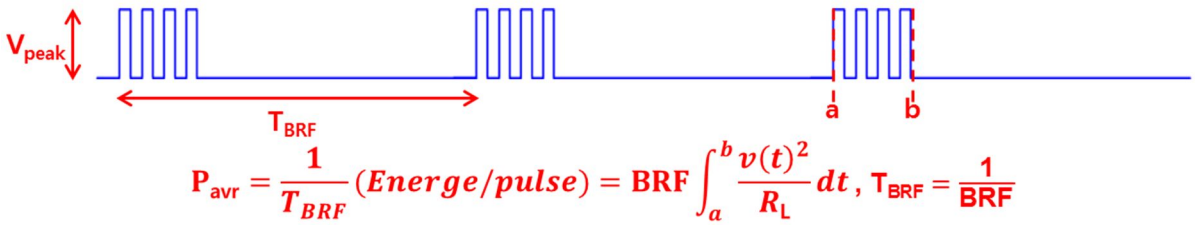

Figure 3-3: Expression of energy/pulse in this thesis.

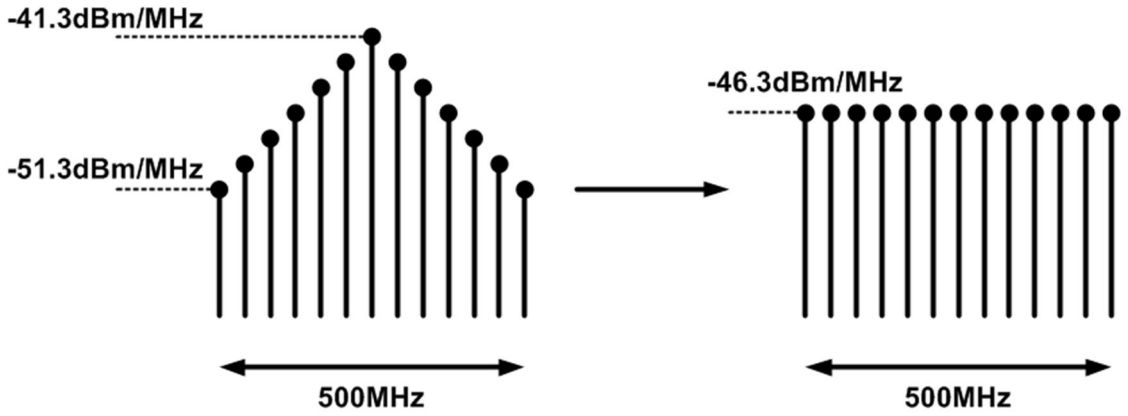

Figure 3-4: The worst case of spectrum characteristic for the output signal.

The output signal power of UWB transmitters has a limitation of -41.3dBm/MHz. Thus, it is necessary to predict the output voltage amplitude before performing real implementation. Assume that output signal has a minimum 10dB bandwidth of 500MHz, and does not include spectrum near DC component, because frequencies located near DC are filtered out before transmission. Thus, V_{peak} is converted to $V_{peak\text{-}to\text{-}peak}$. Let's assume that the amplitudes of V_{peak} and V_{pp} are the same. In ideal situat-

V_{peak} = 0.12 ~ 1.2V (BRF: 1M ~ 32MHz), Z_L = 50Ω,
Output power limitation: -41.3dBm/MHz → -14.3dBm → 37.15uW (the best case)
→ -19.3dBm → 11.75uW (the worst case)

	Channel 1		Channel 2		Channel 3	
	Delay: 1.43102e-10		Delay: 1.25219e-10		Delay: 1.1284e-10	
BRF	Amplitude (V_{worst}) [V]	Amplitude (V_{best}) [V]	Amplitude (V_{worst}) [V]	Amplitude (V_{best}) [V]	Amplitude (V_{worst}) [V]	Amplitude (V_{best}) [V]
1M	0.716	1.2	0.722	1.2	0.722	1.2
2M	0.506	0.901	0.511	0.908	0.510	0.907
4M	0.358	0.637	0.361	0.642	0.361	0.642
8M	0.253	0.450	0.255	0.454	0.255	0.454
16M	0.179	0.318	0.181	0.321	0.180	0.321
32M	0.127	0.225	0.128	0.227	0.128	0.227

Table 3-2: Predicted output voltage according to BRF and channel.

ion, the output signal including frequency component that has uniform value of -41.3dBm within 500MHz, is regarded as the best case. The calculated value is

$$\text{-41.3dBm/MHz} + 10\log 500(\text{MHz}) = \text{-14.3dBm} \rightarrow 37.15\text{uW} \quad (3)$$

The unit, dBm used to evaluate signal power, represents an absolute log-scaled value of milli-watt. Thus, linear-scaled value of signal power can be obtained by taking inverse transformation. The worst case is illustrated in Fig. 3-4. The magnitude of each frequency component within 10dB bandwidth linearly increases or decreases, which is transformed to uniform magnitude of -46.3dBm. And its calculated value is

$$\text{-46.3dBm/MHz} + 10\log 500(\text{MHz}) = \text{-19.3dBm} \rightarrow 11.75\text{uW} \quad (4)$$

When the output power is defined, the output voltage amplitude, V_{peak}, can be calculated in digital architecture as below:

$$V_{peak} = \sqrt{\frac{\text{Output impedance} \cdot P_{out}}{\#\text{ of fine pulses} \cdot \text{Delay time} \cdot \text{BRF}}} \quad (5)$$

Output impedance is 50Ω. P_{out} is the averaged signal power at the output. The number of fine pulses and delay time are different according to a channel used for signal transmission. Table 3-2 shows the -

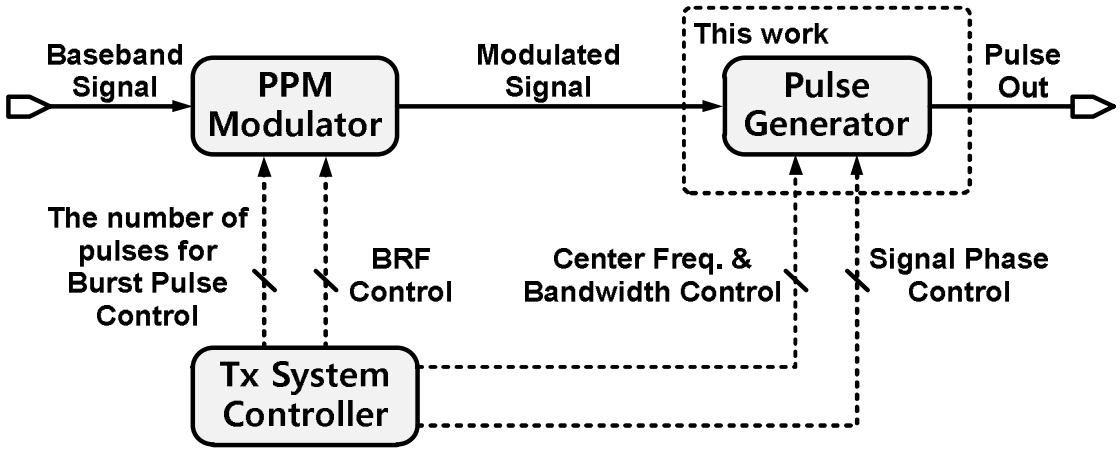

Figure 3-5: System configuration for IR-UWB signal transmission.

values of V_{best} and V_{worst} for each channel and each BRF. In Table 3-2, it is seen that V_{peak} tends to reduce as BRF increases, and V_{peak} may be up to tens of millivolts when BRF goes to 64MHz or 128MHz. However, at the same BRF, the value of V_{peak} corresponding to each channel and each case is sub-equal.

3.2. Entire System Configuration for IR-UWB signal Transmission

In order to accomplish lower power consumption while accommodating the DAA requirement, a novel digital architecture to generate IR-UWB signal, enabling variable channel selection without local oscillator and mixer, is implemented in this thesis. Fig. 3-5 shows the functional block diagram of the IR-UWB signal transmission system. The system consists of modulator, system controller, and pulse generator. BRF is between 1 and 50MHz due to the output power limitation, and directly relates to data throughput. As the number of pulses for burst pulse changes, the output signal power varies even though BRF is fixed. When a certain V_{peak} is given, for example, the averaged power of output signal utilizing BRF of 1MHz, when burst pulse is constructed by 2 fundamental IR-UWB pulses, is the same as that of signal using BRF of 2MHz and a burst pulse including a single IR-UWB pulse. PPM scheme leading to use non-coherent receivers is mainly used for signal transmission. DB-BPSK is additionally employed in the pulse generator block, with a purpose of making the output signal spectrum characteristic more improved. This thesis primarily deals with pulse generator design as the most important subsystem of the transmitter described in Fig 3-5.

3.3. Pulse Generator Architecture

The proposed pulse generator includes several functional blocks. All-Digital Oscillator (ADO), which contains a delay line and an edge combiner, is the block to originate a fundamental IR-UWB si-

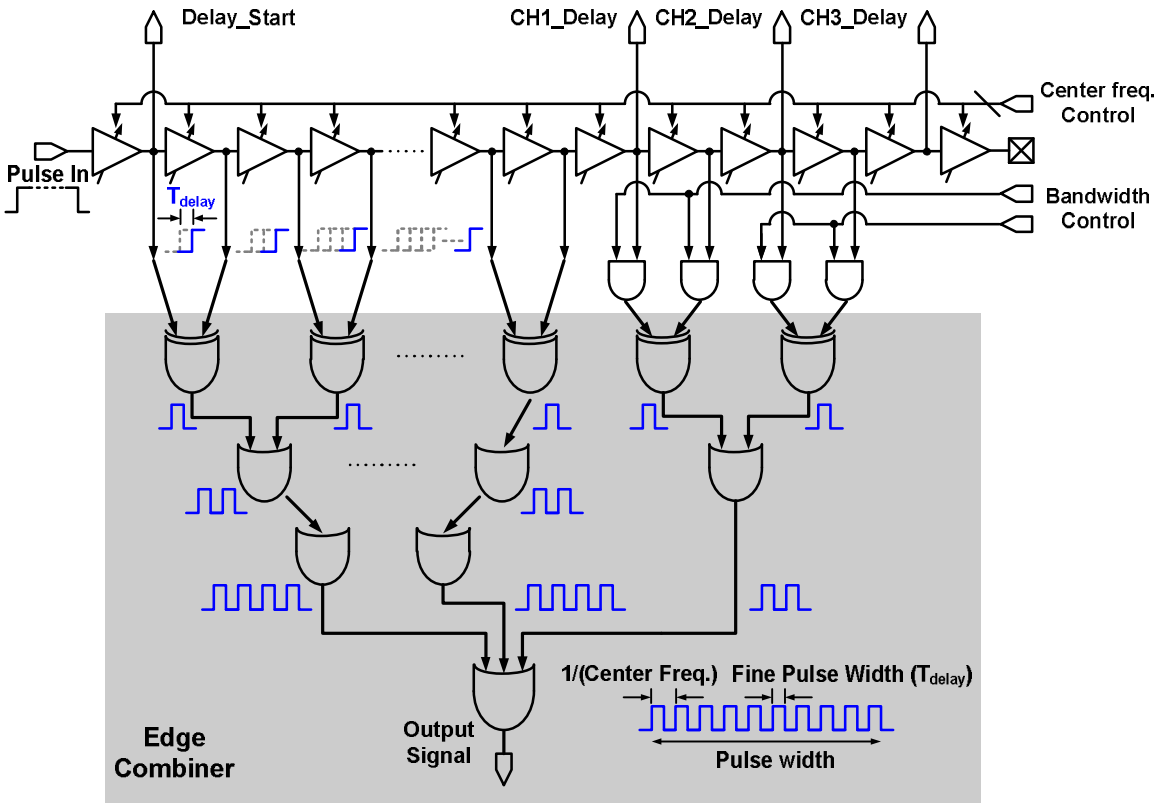

Figure 3-6: ADO block diagram.

gnal. Self-referencing technique for removing unwanted signal and signal phase controlling method for DB-BPSK scheme, as using the output signal of ADO, are also demonstrated in this section.

3.3.1. Fundamental Impulse Generation

ADO is the essential component of IR-UWB system for variable channel selection. The implementation of ADO is directly oriented to the system performance and low cost. It is able to generate signals with the center frequency between 3.5 and 4.5GHz, and the fixed bandwidth of 500MHz. While previous all-digital pulse generators were implemented in 65-nm and 90-nm CMOS process [23], [32], in this thesis, the proposed pulse generator is designed in 0.13-um CMOS process with simplified architecture for lower cost.

The ADO configuration which generates impulse signal is represented in Fig. 3-6. The principle of operation is as follows. When input signal modulated by PPM scheme is applied to the input port, 20 delayed signals are generated from 22 delay cells connected in series. Then, each edge of the delayed signal is transferred to edge combiner and an impulse signal including 10 fine pulses for IR-UWB communication would be composed. ADO basically produces the signals corresponding to each channel, with the delay cells digitally adjusted by 6-bit center frequency control input. 2-bit bandwidt-

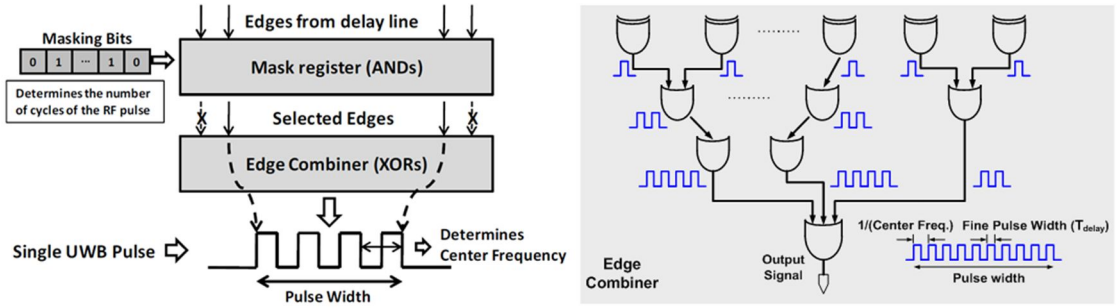

Figure 3-7: XOR-tree and the combination of XOR and OR gates.

h control input can define the number of fine pulses after the center frequency is determined. Because pulse width is related to the number of fine pulses and affects bandwidth of output signal, it is supposed to be approximately 2nsec in order to obtain the bandwidth of 500MHz. Thus, bandwidth can be fixed as channel varies by manipulating the number of fine pulses. Channel 1, 2 and 3 have 8, 9 and 10 fine pulses respectively. Delay_Start, the first delayed point, and the delayed signals corresponding to each channel, CH1_Delay, CH2_Delay and CH3_Delay, are used for DB-BPSK scheme. The relationship among delay time (T_{delay}), center frequency (f_c), bandwidth (BW) and the number of fine pulses (N_{fp}) is expressed as below:

$$f_c = \frac{1}{2 \times T_{delay}} \quad [Hz]$$
$$BW \propto \frac{1}{T_{delay} \times (2 \times N_{fp} - 1)} \quad [Hz] \qquad (6)$$

3.3.2. Edge Combination

While XOR-gate tree is used to perform edge combination in [32], OR-gate is also utilized for the combination of each fine pulse in this thesis. The logical function of OR-gate is as same as XOR-gate after generating one fine pulse as shown in Fig. 3-7. XOR-gate tree needs mask-register and more control bits [32] so that each delayed signal path is symmetric. XOR-gate tree, therefore, is not utilized because asymmetry already exists in ADO including 2 AND-gates used to lead simple architecture for the fixed bandwidth control. Also, this asymmetry would be overcome by adjusting the size of every transistor building each OR-gate. The lower gate count of a stable OR-logic than that of XOR-logic results in lower cost implementation in the same CMOS process.

3.3.3. A Digitally Controlled Delay Cell

Conventional delay cell is supposed to produce two identical delay times for rising and falling edges of a pulse signal. In practice, it is difficult to make such tiny delay times of both edges the same

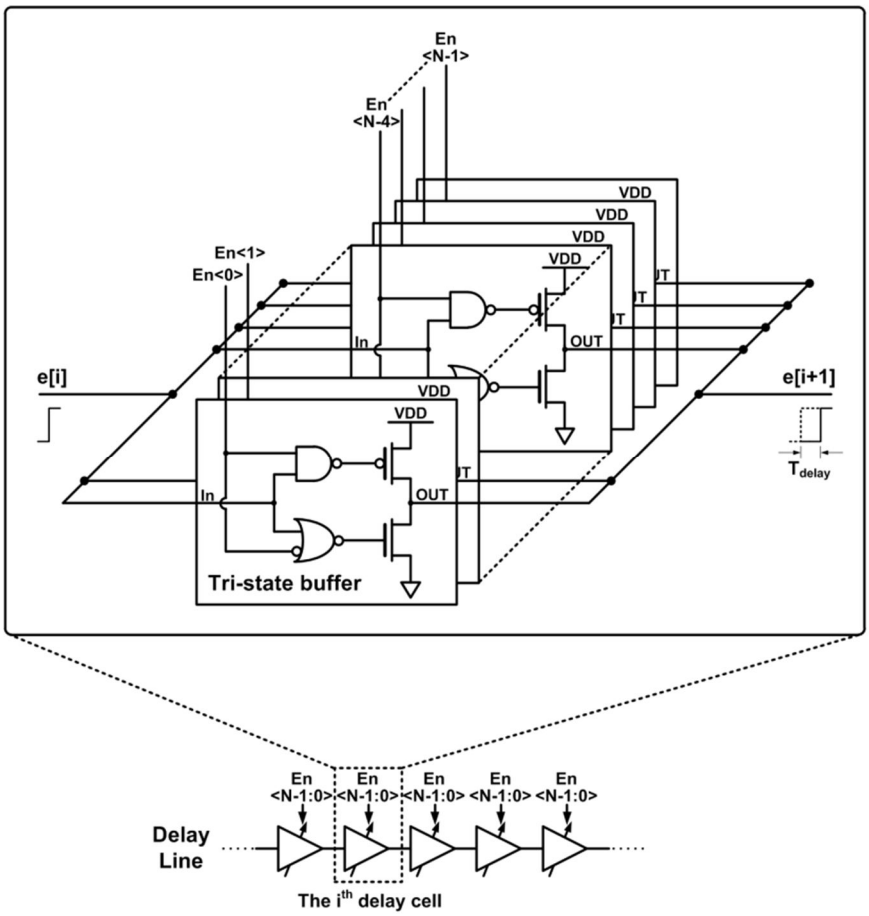

Figure 3-8: Delay cell architecture.

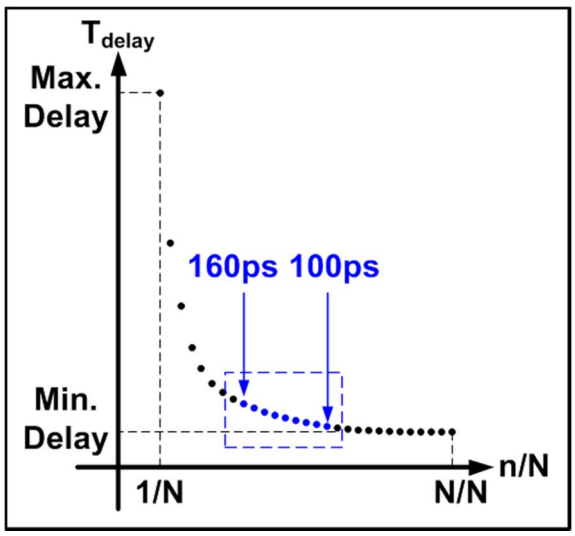

Figure 3-9: The relationship between n/N and delay time.

for high frequency applications. Thus, only the delay of rising edge is exploited to generate IR-UWB signal in 0.13-um CMOS process. Fig 3-8 shows the structure of a delay cell [32] employed in this a -

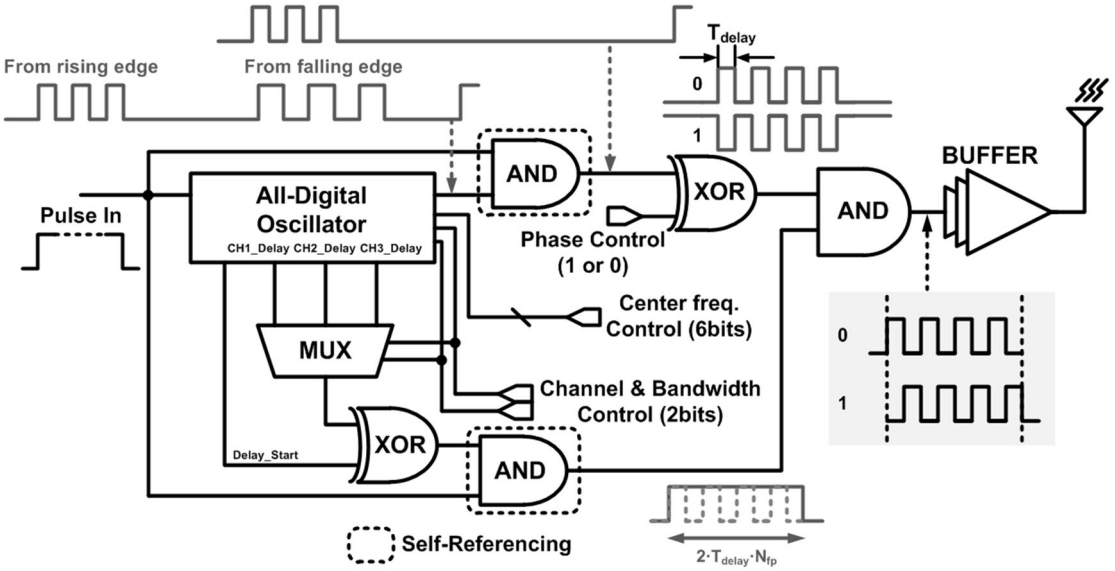

Figure 3-10: The entire block diagram of the proposed pulse generator.

pplication. For simple architecture to be digitally controlled, a delay cell using tri-state buffer [33] was chosen. Each delay cell is composed of the N tri-state buffers which are connected each other in parallel. Pulse signal e[i] is given at the input stage of the i^{th} delay cell, then pulse signal e[i+1] appears at the output stage after a certain time period (T_{delay}) that can be as follows:

$$T_{delay} \propto \frac{(C_1 + C_{adj}) \times N}{n} + C_2 \quad [sec] \tag{7}$$

where N is the total number of tri-state buffers, n is the number of buffers turned on. C_1 and C_2 are the nominal parasitic capacitors when the size of each transistor in a tri-state buffer is assigned [32]. C_{adj} is the adjusted parasitic capacitor intentionally added in layout procedure to make delay time linearly controllable in accordance with each application. The ratio of n to N, n/N, is able to control delay time since it can determine the amount of currents that drives the speed of charging and discharging capacitive components. As depicted in Fig 3-9, the relationship between n/N and T_{delay} is nonlinear. If the frequency range covers whole UWB spectrum, the delay time for low band cannot be clearly adjusted or so many tri-state buffers need to be controlled. Therefore, choosing minimum delay time and finding the proper number of N are the most important procedure for the design of delay cell linearly well operating within a specific range.

3.3.4. Self-Referencing Technique

Self-referencing technique is proposed to remove unwanted signal as shown in Fig. 3-10. When the PPM modulated signal goes into the input of ADO, two impulse signals that have different center fre -

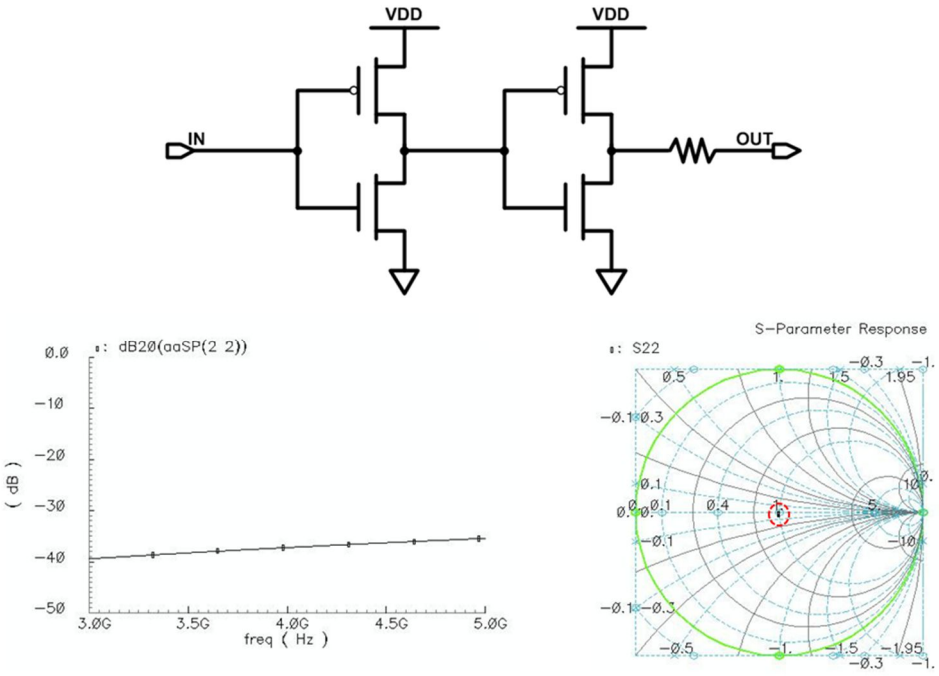

Figure 3-11: Buffer schematic and resistive output matching.

quency and bandwidth each other are generated from rising edge and falling edge at the output of ADO. An AND-gate is applied as a self-referencing technique so as to cancel the impulse signal generated from falling edge. This technique is an effective and simple solution to remove undesirable signals.

3.3.5. Phase-Controlling Technique

In order to reduce spectral line problem, as explained in chapter Ⅱ, DB-BPSK scrambling is implemented in the proposed pulse generator. While the existing technology includes a delay line and a digitally controlled oscillator (DCO) to realize DB-BPSK [34], this thesis presents a new method eliminating the DCO by using only a delay line as illustrated in Fig. 3-10. In the signal path, an XOR-gate is used with self-referenced signal input and 1-bit phase control input to pass or invert the signal from former stage. Delayed signals including Delay_Start, CH1_Delay, CH2_Delay and CH3_Delay from the delay line, are able to produce a supplementary pulse signal for DB-BPSK. Its pulse duration is twice the product of T_{delay} and N_{fp}. The last logical multiplication between two signals from previous stages determines signal phase.

3.3.6. Buffer for 50Ω Output Matching

Power amplifier (PA) is not needed to drive the generated impulse signal to antenna, because the impulse signal already fully swings. Thus, a driver circuit is just demanded to effectively transfer the -

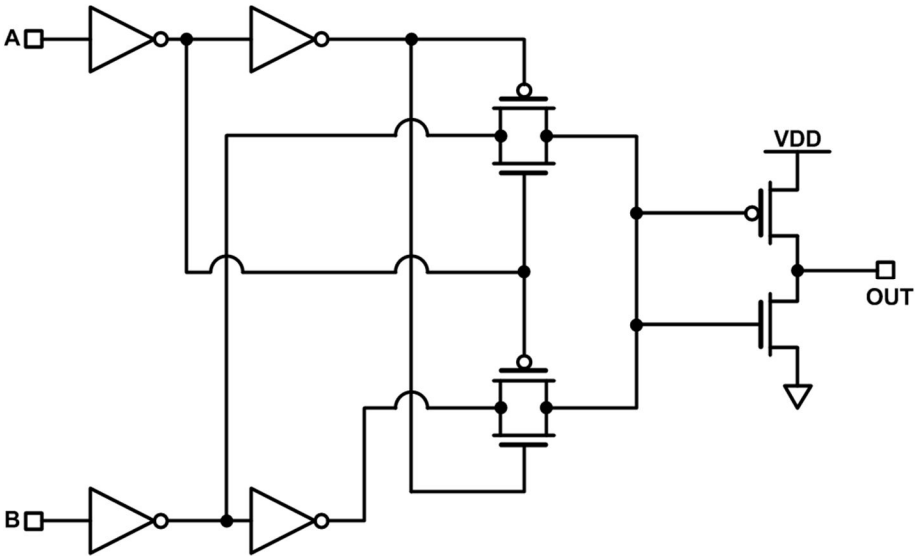

Figure 3-12: XOR gate.

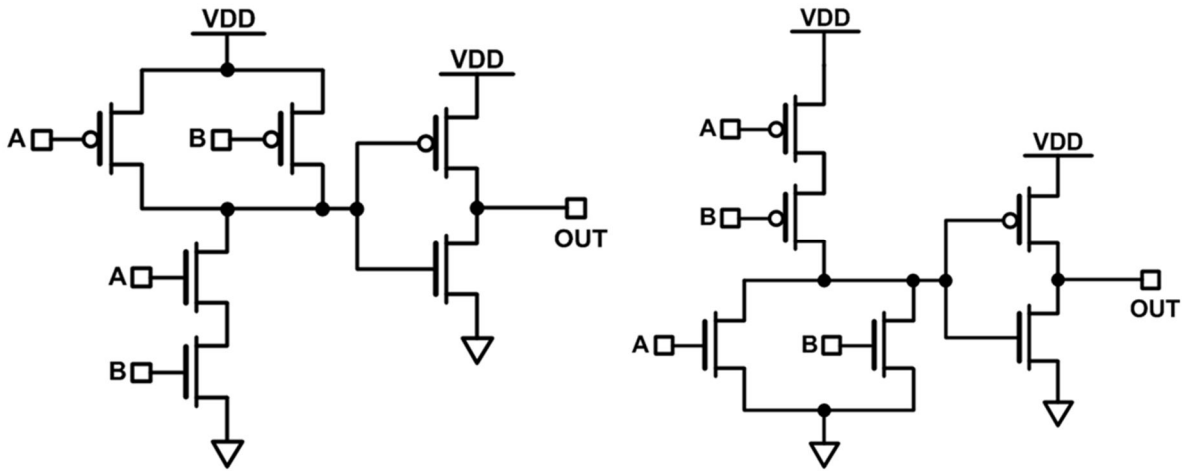

Figure 3-13: OR and AND gates.

UWB signal to antenna. For the implementation of driver circuit, a digital buffer using 2 push-pull inverters is exploited as described in Fig. 3-11. Its input impedance matching can be disregarded. However, output matching to 50Ω is significant for maximum power transfer. Resistive matching is effective way and commonly used for digital circuit. Fig. 3-11 also shows resistive matching technique and result. In general, value of S_{22} under -10dB is enough for output matching.

3.3.7. Logic Gates for Pulse Generator Implementation

Static logic gates, such as AND, OR and XOR logic, are used for the proposed pulse generator. XOR gate is the most important logic gate for edge combination. The outputs of the two interleaved edge combiners are XORed in order to synthesize the final pulse. This XOR was implemented using a

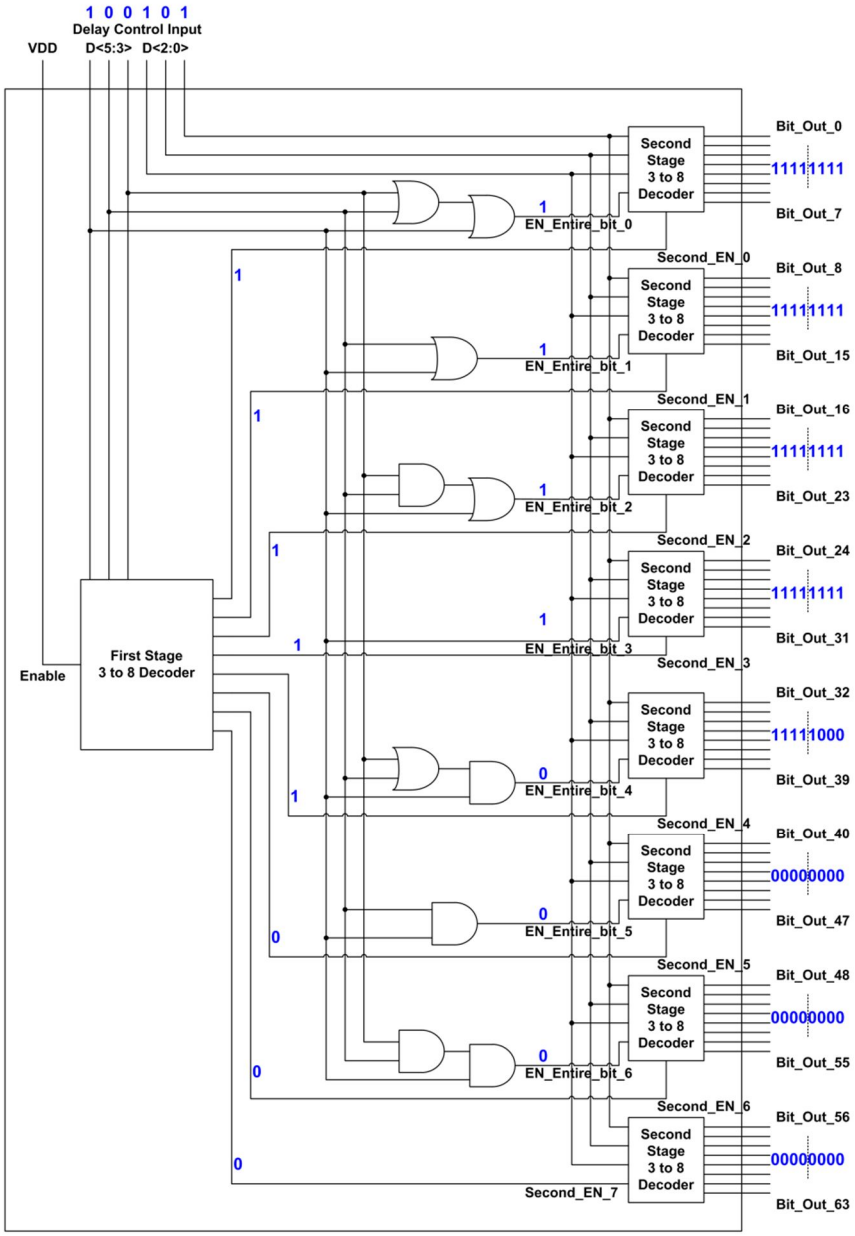

Figure 3-14: A modified 6 to 64 decoder for delay control.

pass-gate topology, which offers the best combination of speed and matched delay paths for a single-ended circuit. A schematic of the XOR is shown in Fig. 3-12. The typical topology using 6 transistors, as shown in Fig. 3-13, is utilized to build OR and AND logic gates.

3.3.8. A Customized 6 to 64 Decoder for Center Frequency Control

Fig. 3-14 and 3-15 show the structure of the delay controller, a modified 6 to 64 decoder, adjusting delay time. The 6-bit delay control input generates the 64 Bit_Out signals in order to determine the operation of each tri-state buffer in a delay cell, and every Bit_Out<63:0> signal corresponds to that -

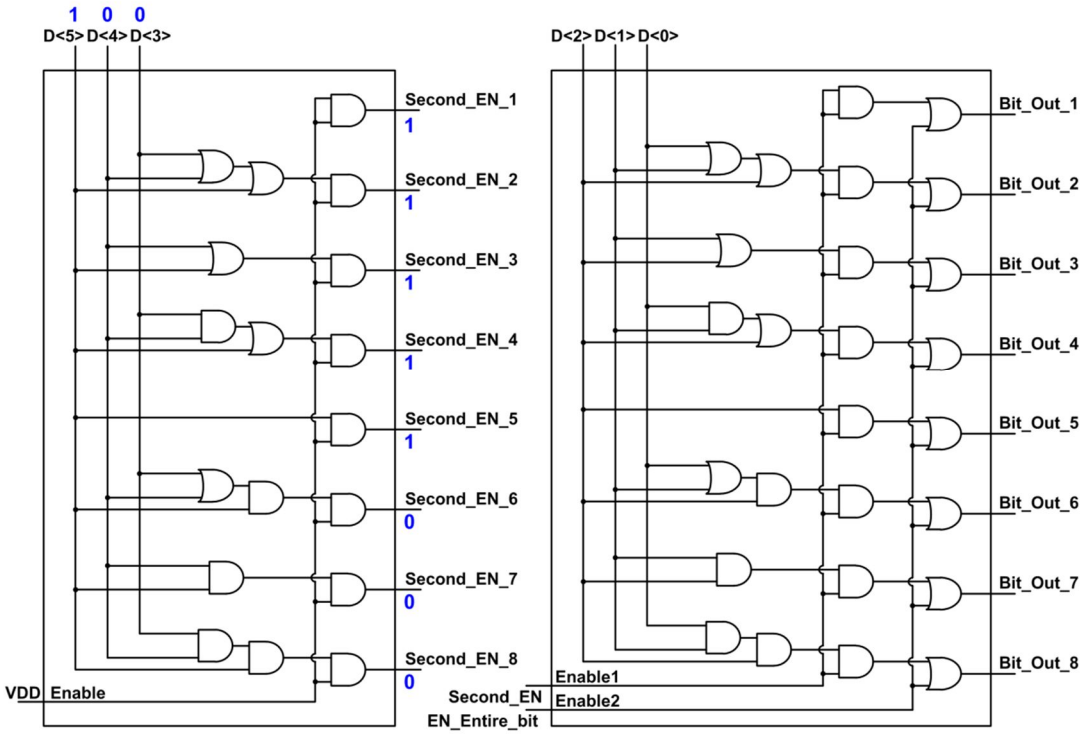

Figure 3-15: 3 to 8 decoders; the first stage (the left), the second stage (the right).

of En<63:0> in Fig. 3-8. The output signals of the first-stage decoder, Second_EN<7:0>, can determine the on/off operation for all the second-stage decoders. EN_Entire_bit<6:0> decides whether to make every output, of each second-stage decoder, logic high or low. Thus, all the second-stage decoders, except the second-stage decoder<7>, have different structure from the first-stage decoder owing to EN_Entire_bit<6:0>. The entire operation of delay controller can be stated with an example:

- D<5:0> signal, delay control input of '100101', is applied to delay controller.
- At the output stage of the first decoder, Second_EN<4:0> signals are turned into '1' and Second_EN<7:5> signals turned into '0' respectively. Hence, only 5 decoders in the second stage can operate.
- The control input D<5:3> can make EN_Entire_bit<3:0> signals change to '1', and EN_Entire_bit<6:4> signals become '0'. Therefore, all the outputs of the second-stage decoder<3:0> have logic high state.
- At the output nodes of the second-stage decoder<4>, D<2:0> control inputs make Bit_Out<36:32> signals go up to high state.
- In the end, 37 tri-state buffers in each delay cell are turned on by Bit_Out<36:0>, while the other tri-state buffers are turned off.

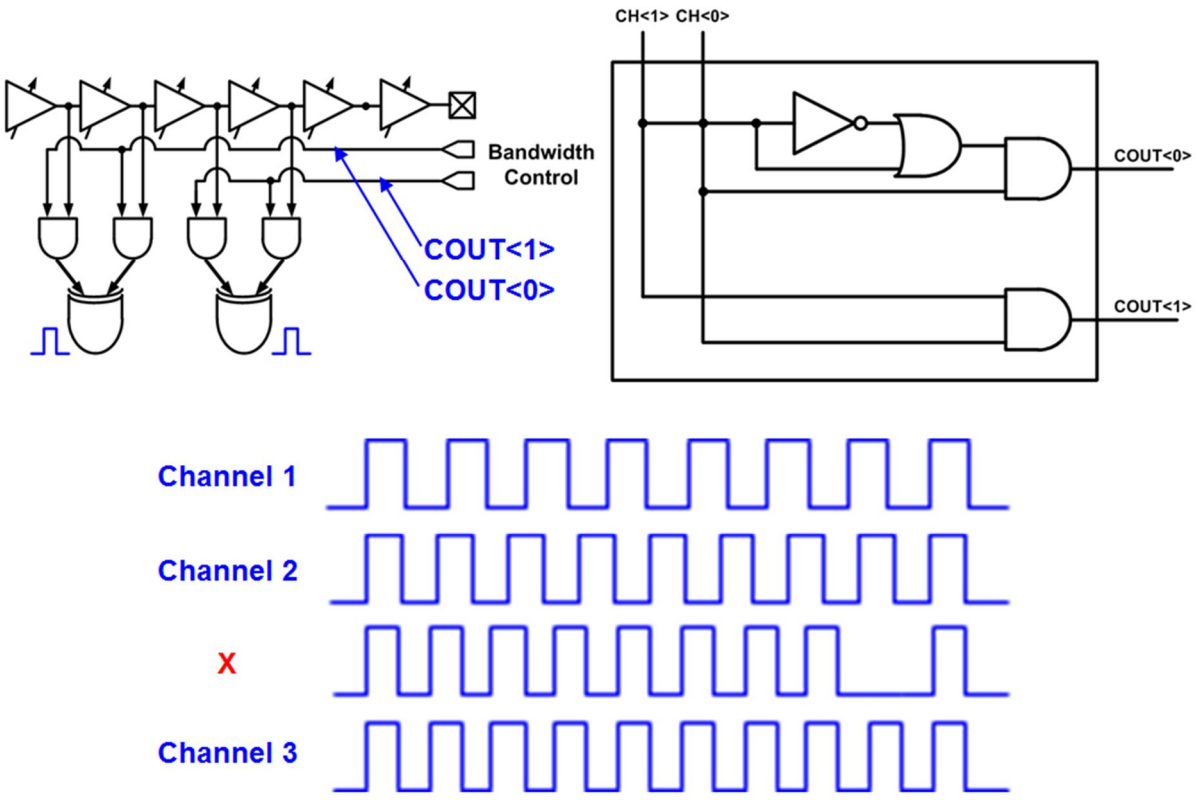

Figure 3-16: The concept of the fixed bandwidth.

CH<1>	CH<0>	COUT<1>	COUT<0>	Channel
0	0	0	0	Channel 1
0	1	0	1	Channel 2
1	0	0	0	Channel 1
1	1	1	1	Channel 3

Table 3-3: The truth table of channel selection.

3.3.9. A Customized 2 to 2 Decoder for the fixed bandwidth

For the fixed bandwidth, 2-bit control input is necessary. However, if we directly apply the control input to the realization of the fixed bandwidth, a signal impossibly used for data transmission, such as changing center frequency, is generated as shown in Fig. 3-16. This phenomenon produces an error for data communication as UWB receiver cannot detect signal representing a data. Thus, in order to remove the undesirable signal generation, a modified 2 to 2 decoder was implemented.

Chapter IV

Design Results

In this chapter, the design results or the characteristics of the system referred in chapter Ⅲ will be discussed. The design is categorized in 2 parts. Each design can be distinguished by DB-BPSK implementation. The first design relates to fundamental impulse signal generation, and the second is the design with signal phase scrambling, DB-BPSK, and exactly the same as the pulse generator stated in chapter Ⅲ. Finally, the system performance is going to be summarized with other pulse generation architecture.

4.1. The First Design Results

The first design was implemented without signal phase scrambling, in order to confirm the fundamental IR-UWB signal generation and variable channel selection capability. All system parameters are intended as explained in Tx system design section. ADO is the core part of IR-UWB transmission system to generate impulse signal, and self-referencing technique was exploited to remove unwanted signal produced from falling edge.

Recall that the basic pulse generation principle is to combine a series of equally-delayed edges to form a single RF pulse, as shown in Figure 4-1. A delay line is used to generate the series of edges from each rising edge of the pulse repetition frequency signal. The edge combination is similar in operation to a frequency multiplier, where the output of the combiner is toggled when an edge is received on any of its inputs. The generated pulse is mathematically equivalent to a baseband square pulse that has been multiplied by a square LO operating at the channel center frequency. The center frequency of the pulse spectrum is varied by controlling the delay-per-stage of the delay line. The width of the pulse is varied by making the number of edges combined programmable. By making both the delay-per-stage and number of edges programmable, the pulse spectrum may be precisely controlled without requiring an RF local oscillator. All blocks, including the buffer to antenna, use full-swing, static CMOS digital circuits, and no analog bias currents are required. The pulse generator is clocked by BRF input, which triggers a single RF pulse on each rising edge of this signal. Each edge of the PRF input propagates through a 21-stage delay line with a 6-bit digitally controlled delay. The 20-edge combiner used to synthesize the IR-UWB pulse by using the combination of XOR and OR gates. The output pulse of ADO is logically multiplied with the input BRF pulse so as to remove the undesirable impulse generated from falling edge, due to its different frequency from rising edge. Finally, the impulse signal is buffered by a digital inverters and its output impedance matched to 50Ω.

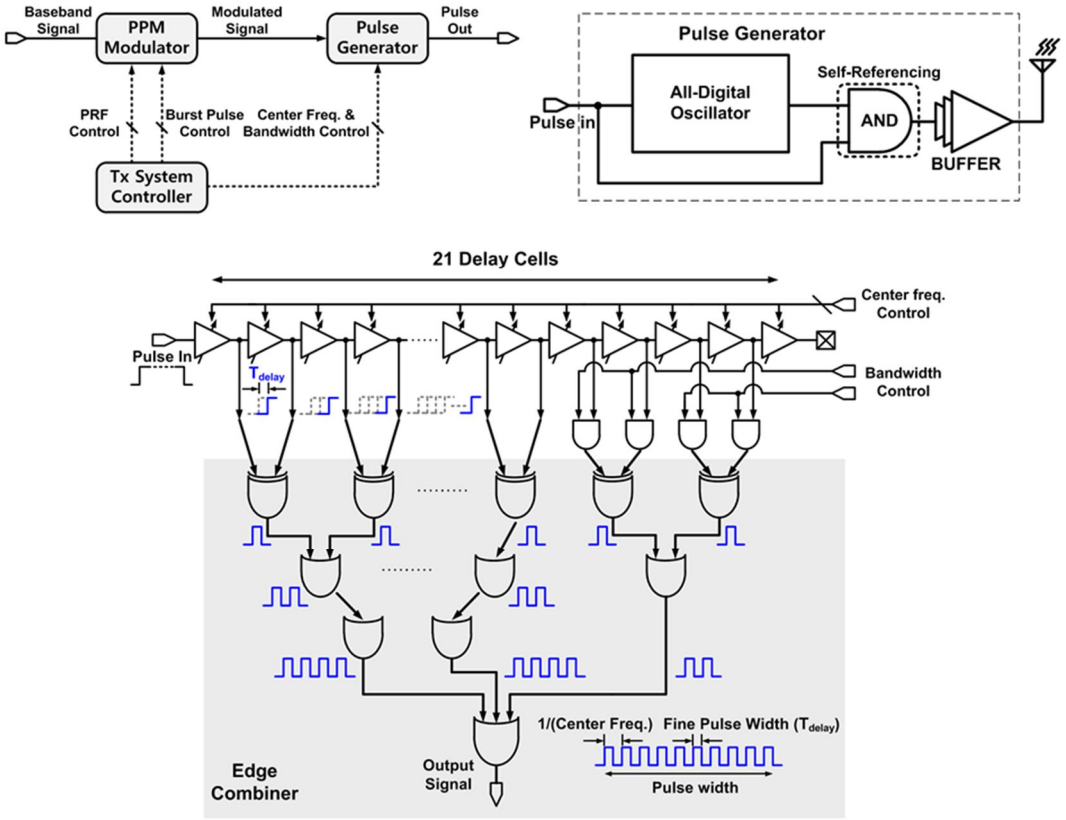

Figure 4-1: The first design: system configuration, pulse generator block diagram, ADO.

Pin name	Default setting	I/O direction	Description
VDD	1.2 V	IN/OUT	DC power supply
GND	0 V	IN/OUT	Connection between Ground & Bulk
BRF_IN	Modulated pulse signal from 1MHz up to 50MHz	IN	Input port With the signal modulated by PPM
D<5:0>	<5:0>=011100	IN	Digital control input port to adjust center frequency
CH<1:0>	00	IN	Digital control input port to adjust bandwidth
IMPULSE_OUT	--	OUT	Signal output port driving up to antenna

Table 4-1: Interface description for the first design.

4.1.1. Interface Description

Totally, 12 pins are required to operate the designed pulse generator. 2 pins are for signal input/output, another 2 pins are for DC power supply, VDD/GND. 8 pins are used to digitally control -

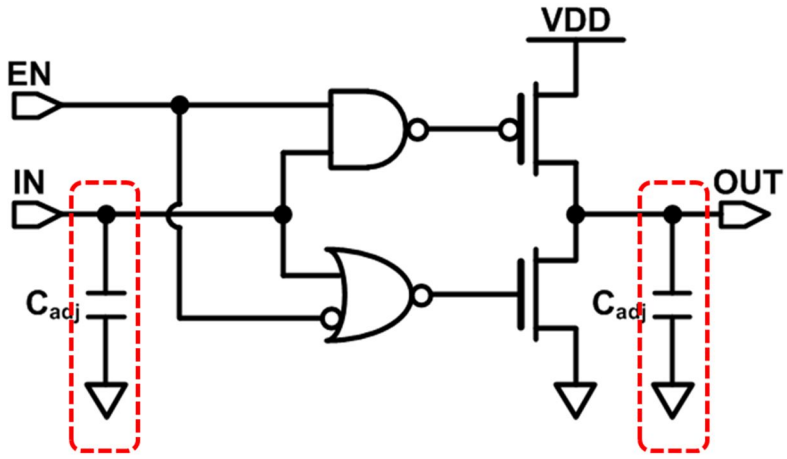

Figure 4-2: Parasitic capacitors in each tri-state buffer.

Specification	Minimum	Typical	Maximum	Units
Supply voltage	1.1	1.2	1.3	V
Temperature	-20	27	80	℃
Parasitic Capacitance at Input/Output, (C_{adj})	3f	7f	11f	F

Table 4-2: The range of variations; supply voltage, temperature, parasitic capacitance.

center frequency and bandwidth. However, the actual minimum number of pins is more than 16pins when considering GSG probe for measurement. In addition, more than 2 pins allocated for each VDD/GND connection can provide more stable power.

4.1.2. Simulation & Layout

4.1.2.1. Simulation Setup

Simulation was taken in Cadence environment with Spectre simulator. The first design was implemented TSMC 0.13-um CMOS process. However, the given PDK for fabrication does not have all corner information. Thus, simulation was run by giving corner information manually as depicted in Table 4-2. Temperature variation, supply voltage variation and parasitic capacitance variation were taken for simulation at the lowest frequency (Channel 1) and the highest frequency (channel 3). Especially, parasitic capacitors (C_{adj}) were given at input/output node in each tri-state buffers, as illustrated in Fig. 4-2, in order to confirm the possibility to control delay time for center frequency even after fabrication. Delay time, pulse shape and amplitude variations were mainly considered in the simulation results.

Results	3f		7f		9f		11f	
	CH1	CH3	CH1	CH3	CH1	CH3	CH1	CH3
Delay time (pico second)	150.372 139.235	110.960	144.254	111.595	144.292	111.727	146.543	111.833
Delay control	001011 001100	011010	011100	101011	100010	110100	101100	111101
Output pulse Amplitude (mV)	489.349	488.913	488.078	487.869	488.813	488.003	487.882	488.141
Output pulse shape	O	O	O	O	O	O	O	O

Table 4-3: Simulation results in the typical case (VDD=1.2V, Temp.=27℃).

			3f		7f		9f		11f	
Voltage (V)	Temp (℃)	Results	$Delay_L$	$Delay_S$	$Delay_L$	$Delay_S$	$Delay_L$	$Delay_S$	$Delay_L$	$Delay_S$
1.1	-20	T_{delay}(ps)	153.337	104.783	160.811	113.355	161.002	114.577	163.763	114.599
		OPA(mV)	439.500	439.160	438.928	439.105	438.540	440.129	439.507	439.655
		OPS(mV)	O	O	O	O	O	O	O	O
	80	T_{delay}(ps)	164.591	111.583	172.424	124.852	172.562	125.727	175.103	125.899
		OPA(mV)	401.256	400.735	401.224	400.000	400.123	399.940	400.500	400.000
		OPS(mV)	O	O	O	O	O	O	O	O
1.3	-20	T_{delay}(ps)	126.784	89.443	134.755	93.494	135.881	93.554	135.895	94.048
		OPA(mV)	582.374	580.000	582.811	580.000	580.874	580.000	582.964	580.000
		OPS(mV)	O	O	O	O	O	O	O	O
	80	T_{delay}(ps)	147.156	101.951	155.731	103.627	156.158	104.908	156.376	104.631
		OPA(mV)	526.711	527.064	526.230	526.000	525.782	529.647	525.557	526.000
		OPS(mV)	O	O	O	O	O	O	O	O

OPA : Output Pulse Amplitude
OPS : Output Pulse Shape (O: stable pulse shape, X: unstable pulse shape)
$Delay_L$: The largest delay time, $Delay_S$: The smallest delay time (in the range adjusted linearly)

Table 4-4: Simulation results with voltage and temperature variations.

4.1.2.2. Simulation Results

Table 4-3 shows the results for typical environment, at VDD of 1.2 volts and at temperature of 27℃. The parasitic capacitance, C_{adj}, was varied from 3f to 11f farads. When C_{adj} is 3f farads, channel 1 can-

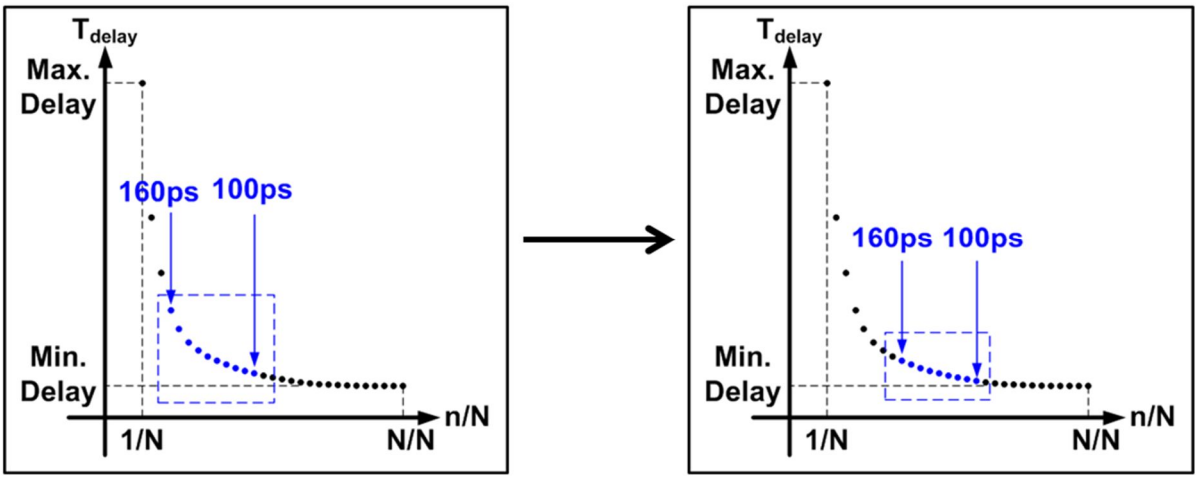

Figure 4-3: The concept of choosing the value of 3f F for C_{adj}.

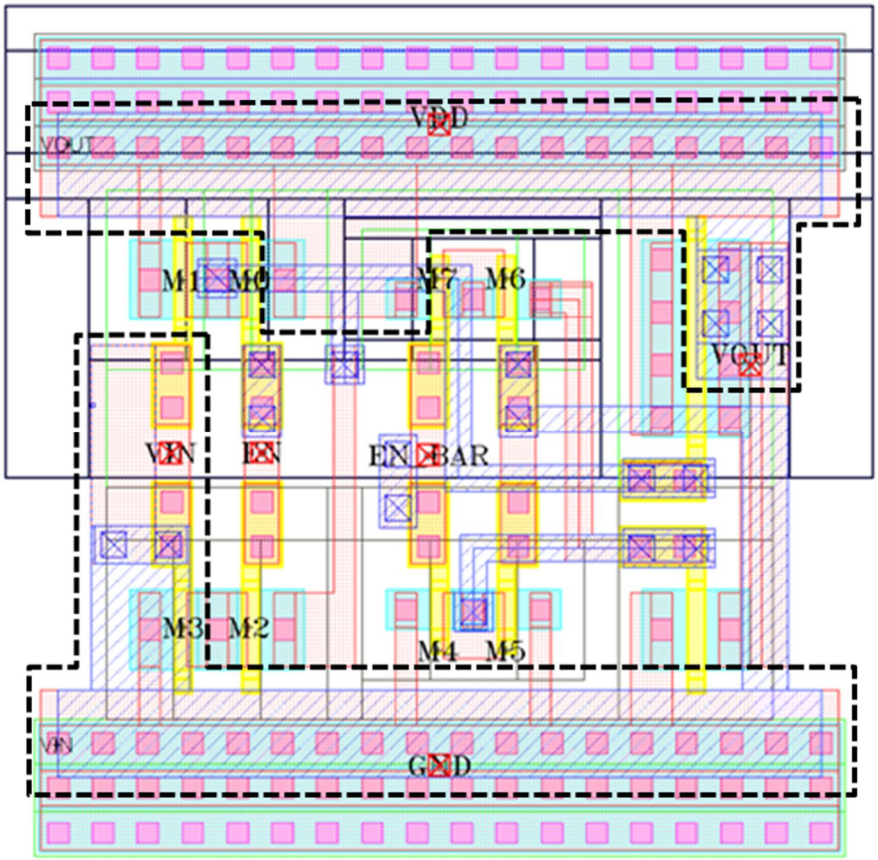

Figure 4-4: A tri-state buffer with the intended parasitic capacitance.

not be realized from the designed pulse generator since its parasitic capacitance is not enough to control such a big delay time. The pulse generator properly operates under the other conditions.

Table 4-4 presents the simulation results with supply voltage variations and temperature variations. $Delay_L$ and $Delay_S$ tell the largest delay time and the smallest delay time respectively, in a linearly co-

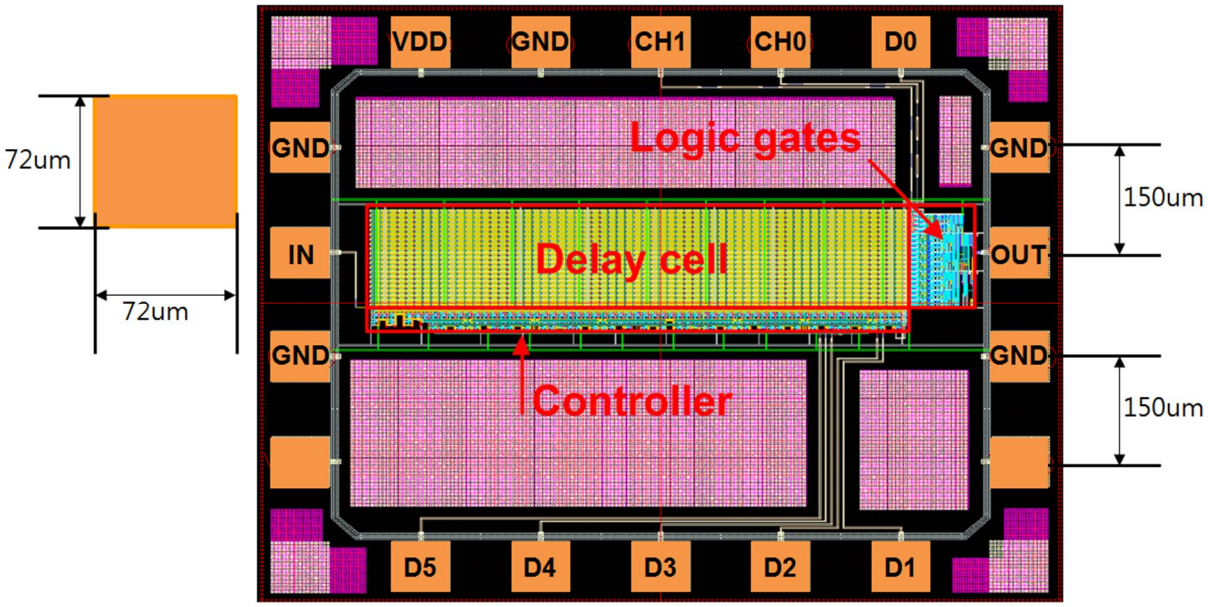

Figure 4-5: System layout.

ntrollable range. At the supply voltage of 1.1 volts, the results under all conditions show the pulse generator does not operate at channel 3 except the condition when C_{adj} is 3f farads. At VDD of 1.3 volts and -20℃, all the simulation results signify that the pulse generator does not operate at channel 1.

As a result, when considering the parasitic capacitance generated during fabrication, C_{adj} of 3f farads can be adopted even though the simulation result at channel 1 is not adjustable to operate. This is because the fabricated parasitic capacitance can make the delay time of the pulse generator well linearly adjustable in a range, and can increase the immunity to the supply voltage variations and temperature variations. The concept is illustrated in Fig. 4-3. Fig. 4-4 shows the layout implementation of a tri-state buffer. Metal plates, including M1 and M2, are added to the input and output nodes, in order to increase parasitic capacitance. The additional parasitic capacitance, 3f farads, was confirmed after RC extraction.

4.1.2.3. System Layout

The entire layout of the design is illustrated in Fig. 4-5. Die size is 1.0 mm x 0.9 mm, the core size is 0.76 mm x 0.15 mm in which 21delay cells occupy the most. The size of pads used here, is 72 um x 72 um with a 150 um pitch. Totally, 16 pins are utilized in this design.

4.1.2.4. Post Layout Simulation

Fig. 4-6 shows the post layout simulation results for a single pulse, including all the parasitic capac-

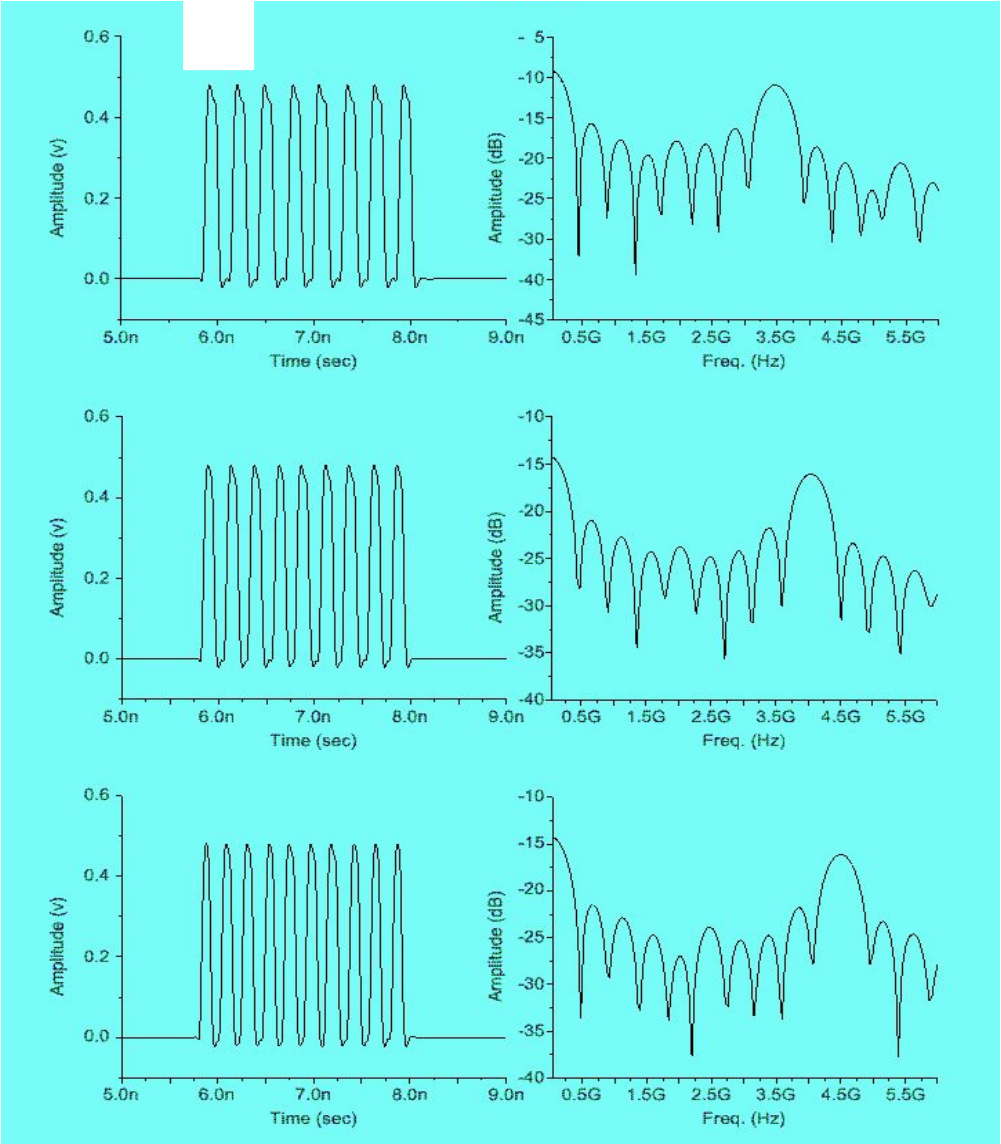

Figure 4-6: Post layout simulation for a single pulse; Channel 1, Channel 2, Channel 3.

itance, inductance and resistance generated in the middle of layout procedure. This simulation contains bond pad and an antenna modeled at 50Ω for closer simulation to the real world. Spectrum analysis does not mean power spectral density (PSD), but presents the relative magnitude between frequencies. Channel 1, 2, 3 have 8, 9, 10 fine pulses respectively. The center frequency for each channel is 3.5GHz, 4GHz and 4.5GHz deliberately. All signals in Fig. 4-6 have pulse width, which is close to 2nsec, and 10dB bandwidth of much more than 500MHz.

4.1.3. Measurement Results

The proposed pulse generator for the first time, was fabricated in a standard 0.13-um CMOS technology with a supply voltage of 1.2 volts. All measurement results were taken from bare chips; a -

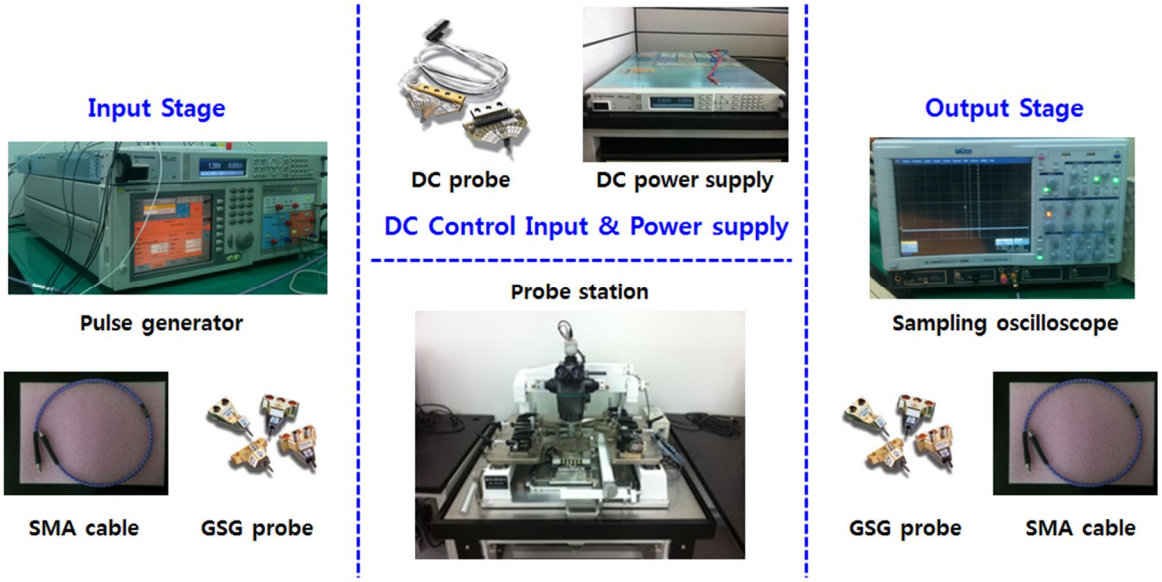

Figure 4-7: Measurement setup for the results in time domain.

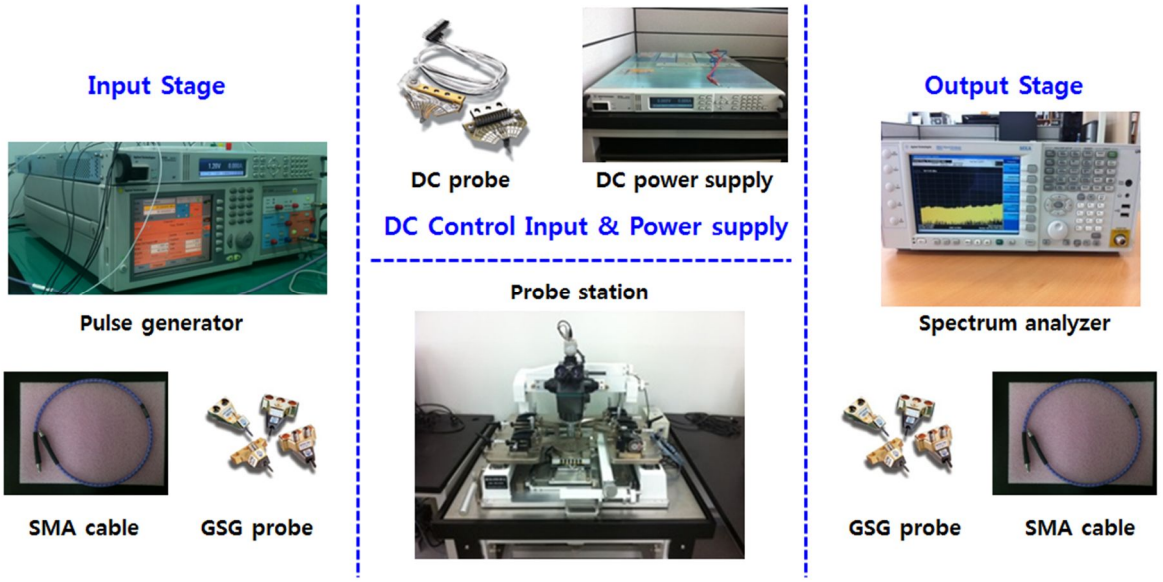

Figure 4-8: Measurement setup for the results in frequency domain.

sampling oscilloscope in Fig. 4-7 is used to confirm signals in time domain, and power spectral density (PSD) was measured by a spectrum analyzer with 1MHz resolution bandwidth in Fig. 4-8.

The transient results at the output node matched to 50Ω are illustrated in Fig. 4-9, and it describes the measured result of the transmitted signal after passing off-chip bandpass filter. The signal in time domain confirms that pulse width is approximately 2nsec as designed. Fig. 4-10 exhibits the measured spectrum for the three channels satisfying FCC mask. 10dB bandwidth for each channel is close to 500MHz as expected. The chip photograph with die size of 1.0 mm x 0.9 mm, is shown in Fig. 4-11. -

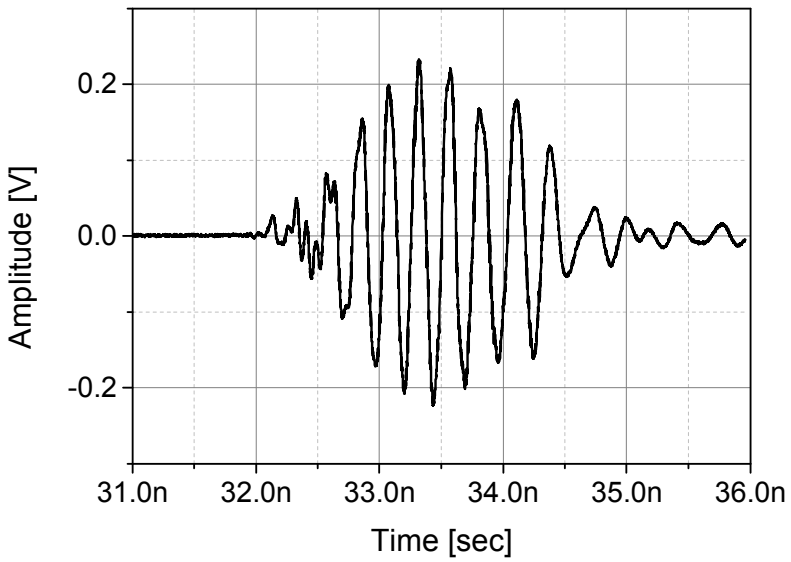

Figure 4-9: Measured results in time domain.

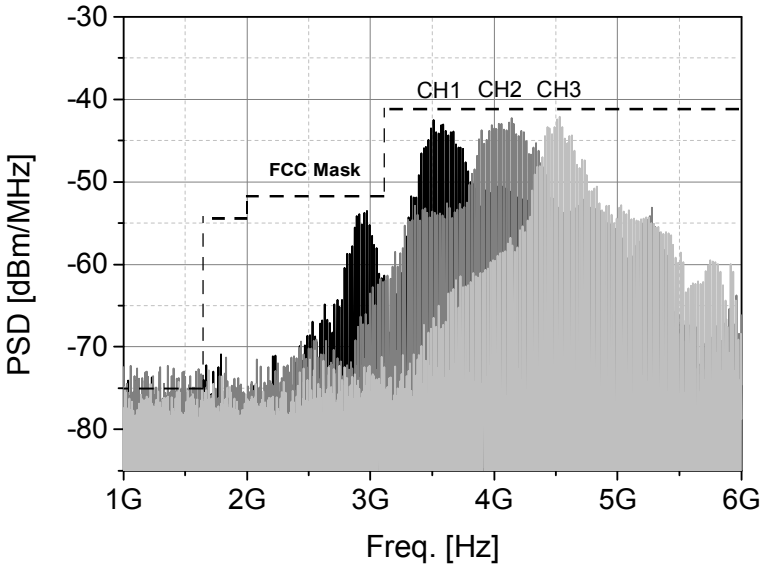

Figure 4-10: Measured results in frequency domain.

The chip was implemented as designed in layout procedure.

4.2. The Second Design Results

The first design is to confirm the fundamental IR-UWB signal generation with variable channel selection. The second design is a technique to give a random signal phase scrambling, DB-BPSK for -

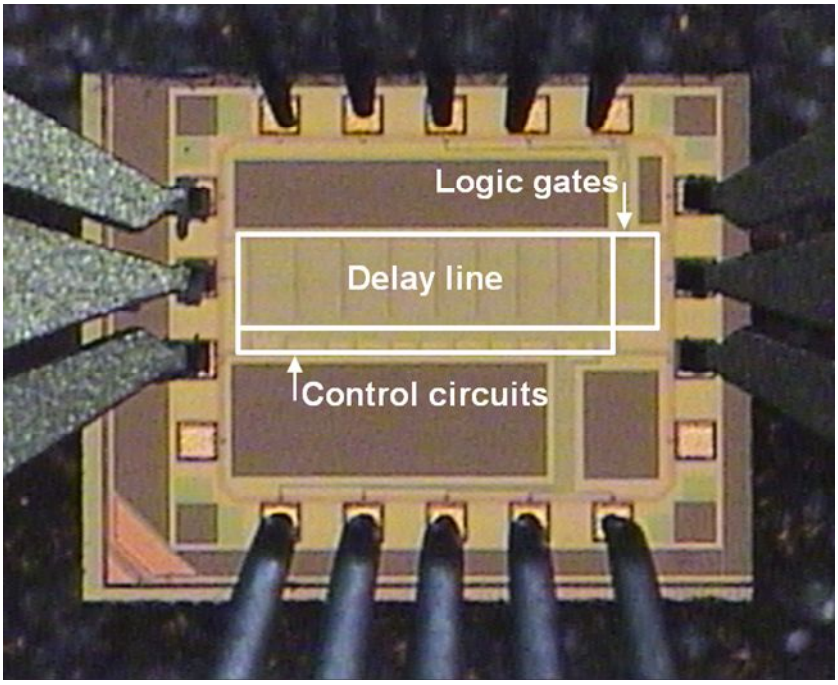

Figure 4-11: Chip photograph.

better spectrum characteristic, to the system designed for the first time. The second design is structured as explained in system design section.

Recall that the reason why using DB-BPSK scrambling. BPSK modulation typically comes with a certain amount of added complexity and power consumption in the transmitter. This complexity often leads to the use of RF amplifiers and mixers dissipating static power, or passive components that consume a relatively large die area. Power and area are two key constraints for which circuit designers go to great lengths to minimize, often at the expense of performance. PPM transmitters and receivers, however, offer an advantage in system complexity over BPSK. Pulse generation circuits become much simpler, and a relatively low power and precision, non-coherent receiver can be used for demodulation. It would therefore be advantageous from a spectrum scrambling and cost perspective to combine the spectral properties of BPSK signals with the implementation simplicity of a PPM transmitter. This can be achieved with the proposed delay-based binary phase shift keying (DB-BPSK) modulation.

4.2.1. Interface Description

Totally, 13 pins are required to operate the designed pulse generator. 2 pins are for signal input/output, another 2 pins are for DC power supply, VDD/GND. 9 pins are used to digitally control center frequency, bandwidth and output signal phase. However, the actual minimum number of pins is

Pin name	Default setting	I/O direction	Description
VDD	1.2 V	IN/OUT	DC power supply
GND	0 V	IN/OUT	Connection between Ground & Bulk
BRF_IN	Modulated pulse signal from 1MHz up to 50MHz	IN	Input port With the signal modulated by PPM
D<5:0>	<5:0>=011100	IN	Digital control input port to adjust center frequency
CH<1:0>	00	IN	Digital control input port to adjust bandwidth
PHASE	0	IN	Digital control input port to adjust output signal phase
IMPULSE_OUT	--	OUT	Signal output port driving up to antenna

Table 4-5: Interface description for the second design.

more than 17 pins when considering GSG probe for measurement. The function for each pin is described in Table 4-5.

4.2.2. Signal Flow

In order to confirm the design validity, the signal at each node is described in Fig. 4-12, as follows:

1) The input signal modulated by PPM modulation scheme.
2) The generated delayed signals.
3) The fine pulses produced by XOR gate.
4) The signals combined by fine pulses, using OR-gate.
5) The output of ADO.
6) The self-referenced signal before/after AND-gate in signal path.
7) The supplementary pulse for DB-BPSK scrambling, using Delay_Start, CH1_Delay, CH2_Delay and CH3_Delay.
8) The fundamental and inverted signal before/after XOR-gate.
9) The output signal of the proposed pulse generator.

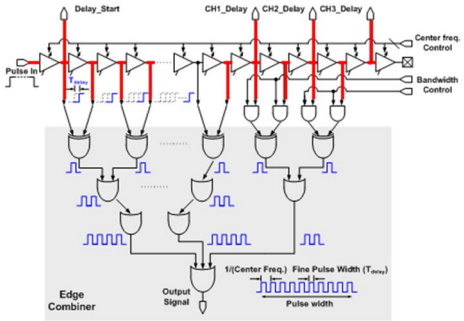
Delay_Start
CH1_Delay
CH2_Delay
CH3_Delay
Center freq. Control
Bandwidth Control
Pulse In
Edge Combiner
Output Signal
1/(Center Freq.)
Fine Pulse Width
Pulse width

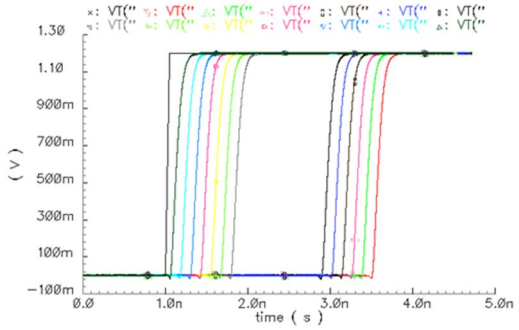
1.3Ø
1.1Ø
9ØØm
7ØØm
5ØØm
3ØØm
1ØØm
−1ØØm
(V)
Ø.Ø
1.Ø n
2.Ø n
3.Ø n
4.Ø n
5.Ø n
time (s)

(a)

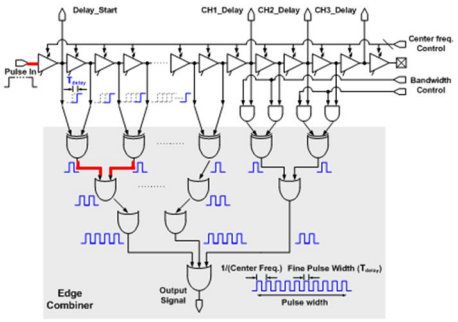
Delay_Start
CH1_Delay
CH2_Delay
CH3_Delay
Center freq. Control
Bandwidth Control
Pulse In
Edge Combiner
Output Signal
1/(Center Freq.)
Fine Pulse Width
Pulse width

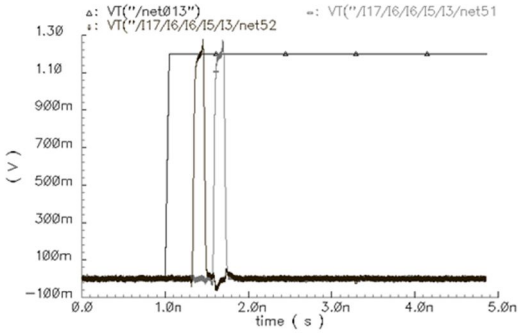
VT("/net013")
VT("/117/16/16/15/13/net52
VT("/117/16/16/15/13/net51
1.3Ø
1.1Ø
9ØØm
7ØØm
5ØØm
3ØØm
1ØØm
−1ØØm
(V)
Ø.Ø
1.Ø n
2.Ø n
3.Ø n
4.Ø n
5.Ø n
time (s)

(b)

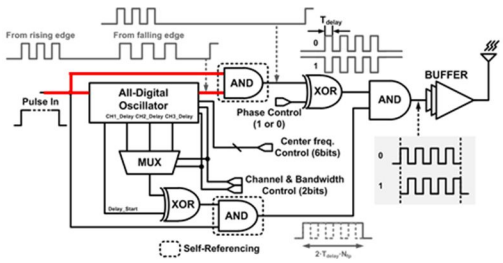
From rising edge
From falling edge
Pulse In
All-Digital Oscillator
AND
XOR
AND
BUFFER
Phase Control (1 or 0)
Center freq. Control (6bits)
MUX
Channel & Bandwidth Control (2bits)
XOR
AND
Self-Referencing

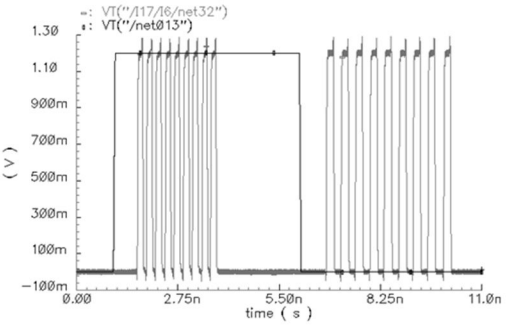
VT("/117/16/net32")
VT("/net013")
1.3Ø
1.1Ø
9ØØm
7ØØm
5ØØm
3ØØm
1ØØm
−1ØØm
(V)
Ø.ØØ
2.75n
5.5Øn
8.25n
11.Øn
time (s)

(c)

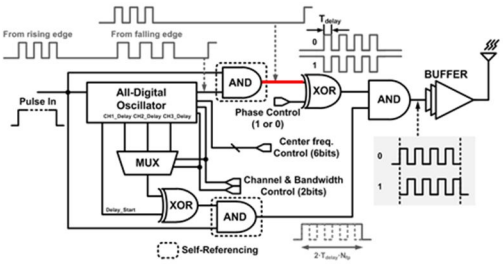
From rising edge
From falling edge
Pulse In
All-Digital Oscillator
AND
XOR
AND
BUFFER
Phase Control (1 or 0)
Center freq. Control (6bits)
MUX
Channel & Bandwidth Control (2bits)
XOR
AND
Self-Referencing

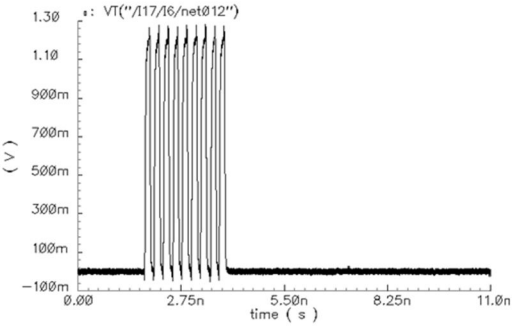
VT("/117/16/net012")
1.3Ø
1.1Ø
9ØØm
7ØØm
5ØØm
3ØØm
1ØØm
−1ØØm
(V)
Ø.ØØ
2.75n
5.5Øn
8.25n
11.Øn
time (s)

(d)

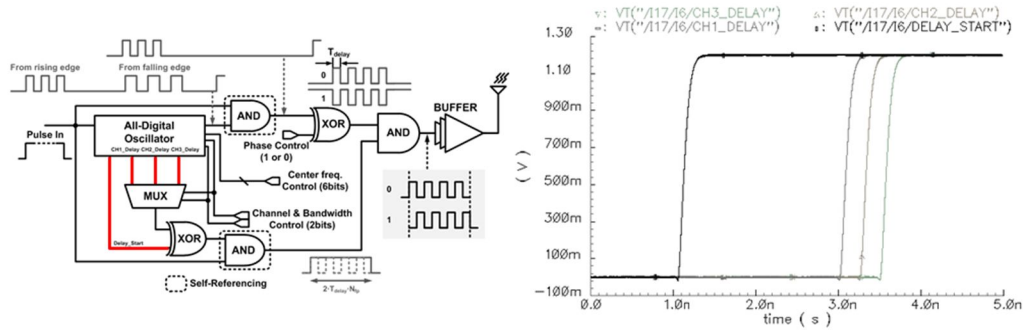
From rising edge
From falling edge
Pulse In
All-Digital Oscillator
AND
XOR
AND
BUFFER
Phase Control (1 or 0)
Center freq. Control (6bits)
MUX
Channel & Bandwidth Control (2bits)
XOR
AND
Self-Referencing
VT("/I17/I6/CH3_DELAY")
VT("/I17/I6/CH2_DELAY")
VT("/I17/I6/CH1_DELAY")
VT("/I17/I6/DELAY_START")
1.3Ø
1.1Ø
900m
700m
500m
300m
100m
−100m
(V)
0.0
1.0n
2.0n
3.0n
4.0n
5.0n
time (s)

(e)

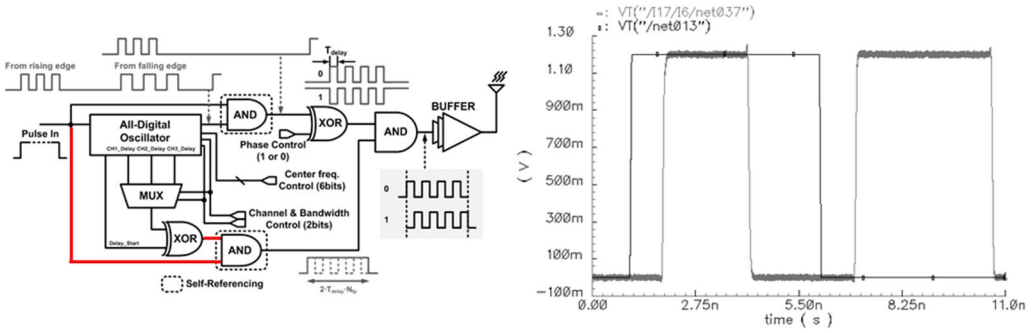
From rising edge
From falling edge
Pulse In
All-Digital Oscillator
AND
XOR
AND
BUFFER
Phase Control (1 or 0)
Center freq. Control (6bits)
MUX
Channel & Bandwidth Control (2bits)
XOR
AND
Self-Referencing
VT("/I17/I6/net037")
VT("/net013")
1.3Ø
1.1Ø
900m
700m
500m
300m
100m
−100m
(V)
0.00
2.75n
5.50n
8.25n
11.0n
time (s)

(f)

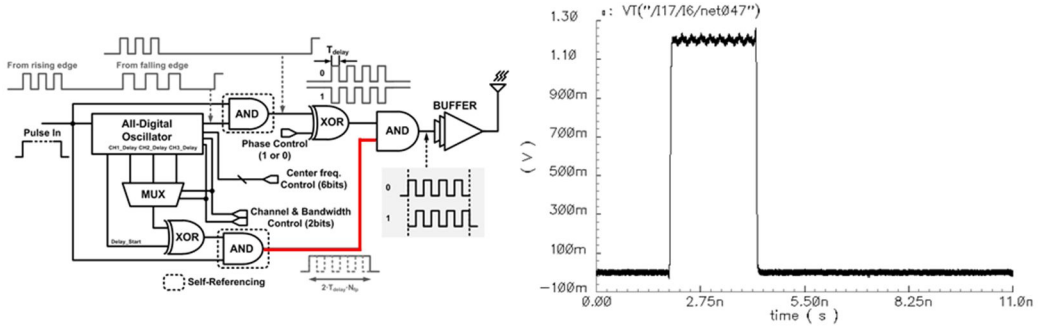
From rising edge
From falling edge
Pulse In
All-Digital Oscillator
AND
XOR
AND
BUFFER
Phase Control (1 or 0)
Center freq. Control (6bits)
MUX
Channel & Bandwidth Control (2bits)
XOR
AND
Self-Referencing
VT("/I17/I6/net047")
1.3Ø
1.1Ø
900m
700m
500m
300m
100m
−100m
(V)
0.00
2.75n
5.50n
8.25n
11.0n
time (s)

(g)

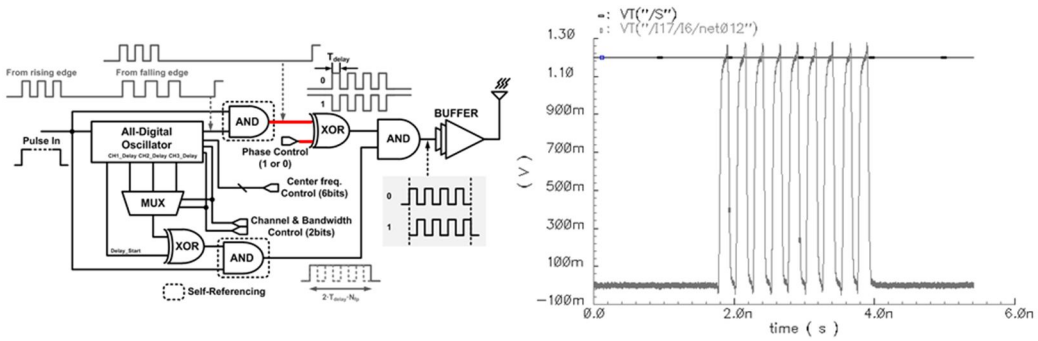
From rising edge
From falling edge
Pulse In
All-Digital Oscillator
AND
XOR
AND
BUFFER
Phase Control (1 or 0)
Center freq. Control (6bits)
MUX
Channel & Bandwidth Control (2bits)
XOR
AND
Self-Referencing
VT("/S")
VT("/I17/I6/net012")
1.3Ø
1.1Ø
900m
700m
500m
300m
100m
−100m
(V)
0.0
2.0n
4.0n
6.0n
time (s)

(h)

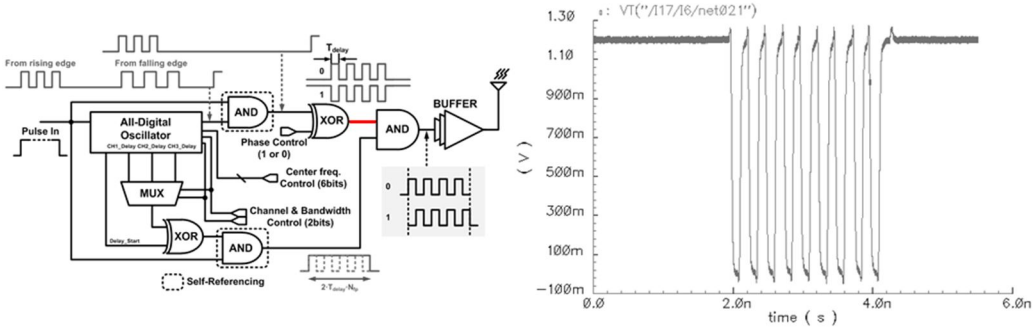

(i)

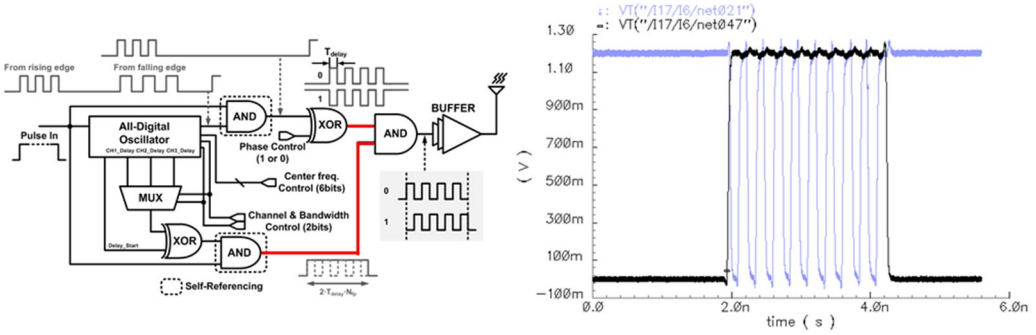

(j)

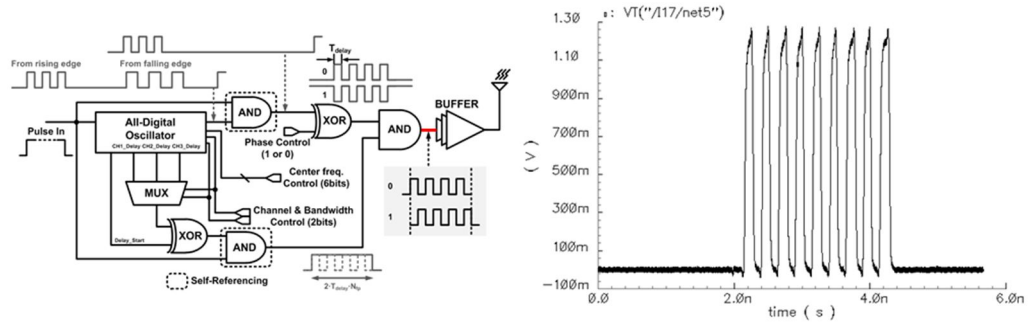

(k)

Figure 4-12: The signal at each node.

4.2.3. Simulation Results

The simulation in time domain was run in Cadence environment with Spectre simulator. And the power spectral density (PSD) simulation was taken in Agilent advanced design system (ADS), with a pulse train modulated by PPM/PPM+DB-BPSK and extracted from Spectre. The second design was also implemented TSMC 0.13-um CMOS process. This simulation is for the typical environment.

The transient results at the output node matched to 50Ω are illustrated in Fig. 4-13 when phase con-

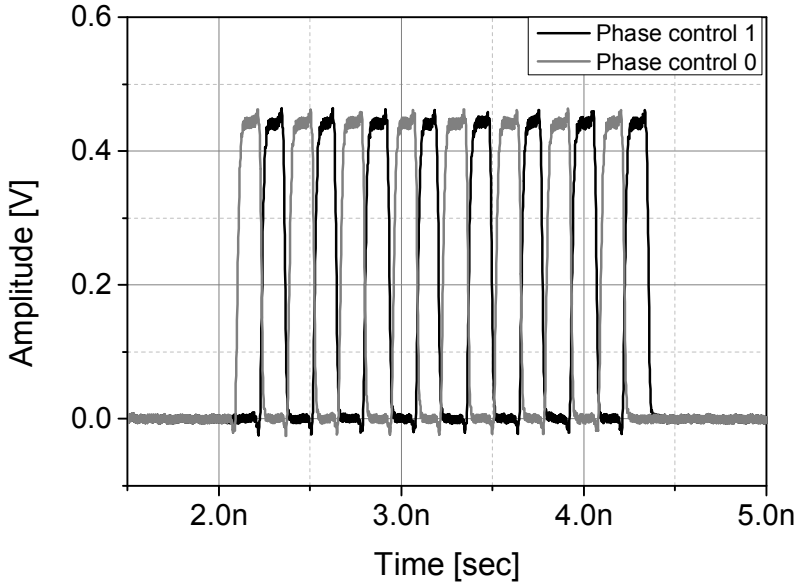

Figure 4-13: Output signals with phase control at channel 1.

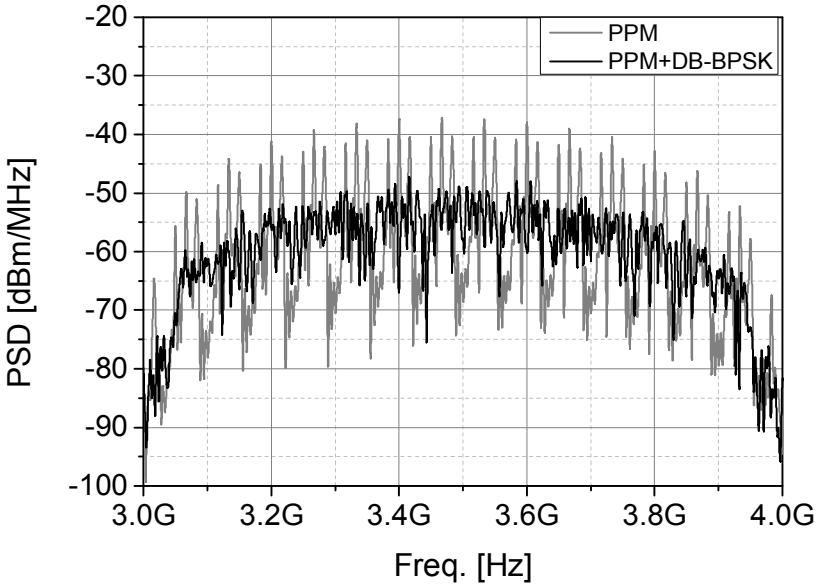

Figure 4-14: Spectrum comparison between PPM and PPM with DB-BPSK.

trol is 0 or 1 at channel 1, and their pulse width is close to 2nsec as designed. Fig. 4-14 shows the difference of PSD characteristic between PPM modulated signal and phase scrambled signal. The picture can clearly describe that the spectrum modulated by PPM with DB-BPSK shows much smaller gap between the peak spectral lines and others when comparing to the PPM modulated signal, leading more effectively utilized signal power.

	[35]	[36]	[37]	[34]	This work
Technology	CMOS 0.13um	CMOS 90nm	CMOS 90nm	CMOS 65nm	CMOS 0.13um
Max. BRF	5MHz	10MHz	15.6MHz	50MHz	50MHz
Frequency Range	7.25-8.5GHz	2.9-3.8GHz	3.1-5.7GHz	3.1-5GHz	3.1-4.8GHz
Pulse Bandwidth	1.25GHz	0.5GHz	~0.5GHz	0.5-1.4GHz	~0.5GHz
Modulation	PPM	OOK	PPM + BPSK	PPM + DB-BPSK	PPM + DB-BPSK
Energy consumption	186pJ/pulse	80pJ/pulse	17.5pJ/pulse	12pJ/pulse	48pJ/pulse

Table 4-6: Performance summary.

4.3. Performance Summary

The performance of the designed pulse generator in this thesis is summarized with other pulse generation structures in Table 4-6. It is difficult to directly compare each methodology due to implementations in different CMOS processes and various specifications. The architecture in [34], for example, shows the lowest energy consumption. However, the cost of fabrication in 65-nm CMOS process is typically much more than that of 0.13-um CMOS process. The cost and power matrix puts this work among the best so far published.

Chapter V

Future Works

UWB radios for low data rate applications such as wireless body area network (WBAN) remain active area of research. In this chapter, the supplement point of the proposed pulse generator and the receiver corresponding to the designed transmission system in this thesis are stated.

5.1. Output Power Control Technique

In order to meet FCC's radiated power limitation, DAA requirement and variable data rate according to transmission distance, Output power control block is required. Energy efficient architecture and the function of adjusting linear-in-dB power are recommended for that block. A pad driver in [23] is described in this section as an example.

An RF pad driver as a final stage in a UWB transmitter in Fig. 5-1, is essentially a digital inverter with added functionality for varying the gain and reducing leakage. The transistors were sized in order to maximize the efficiency of the driver when driving a 50Ω antenna. Because the transistors are large, leakage is a concern in the final stage. A well-known technique of stacking NMOS devices was used in order to reduce leakage. In this case, the stacked NMOS transistors resulted in a leakage current 5 times lower than a single NMOS device for equal pull-down strengths. This is due to the intermediate node between transistors floating higher, increasing the threshold voltage of the top transistor due to the body effect.

A schematic of the driver is shown in Fig. 5-1. During pulse operation, the final stage is essentially a digital inverter formed by a strong PMOS pull-up (MP1) and the stacked NMOS pull-down network. The power of the output pulse is varied by increasing the drive strength of the pull-down network through the digital Gain<6:0> controls. The widths of the NMOS devices in each of the branches of the pull-down network are weighted in order to produce a linear-in-dB power adjustment as shown in Fig. 5-2. During the idle period between pulses, the output node of the transmitter is strongly pulled to VDD through MP1. The driver incorporates a high-impedance standby mode, where the output is pulled to VDD through MP2, which is a weak device. The output is weakly held high in order to eliminate transients that would otherwise occur when coming out of standby mode.

5.2. UWB Receiver Corresponding to The Designed Pulse Generator

The UWB receiver that will be designed for the aspect of low power consumption is based on a dir-

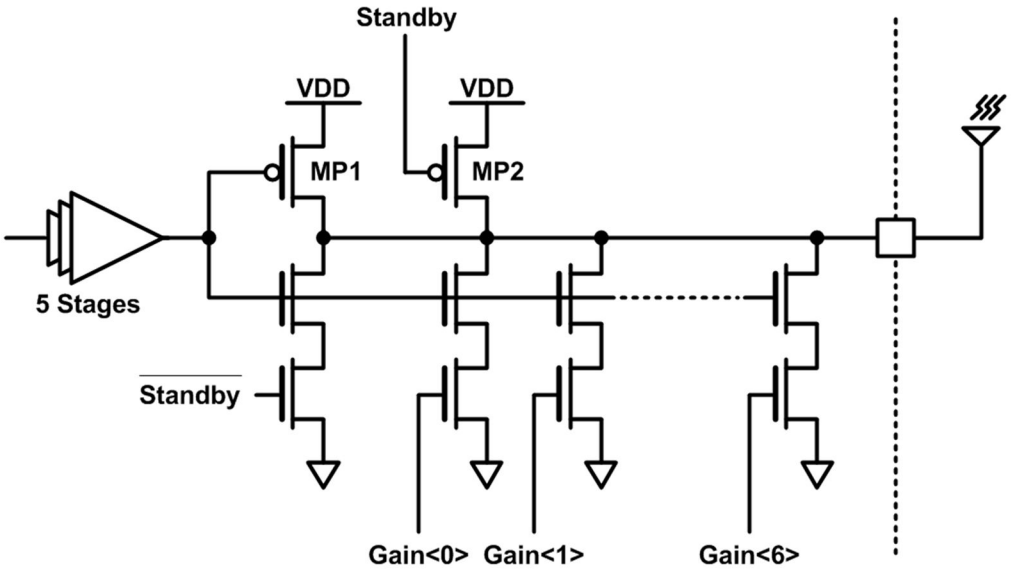

Figure 5-1: An example of output power control technique.

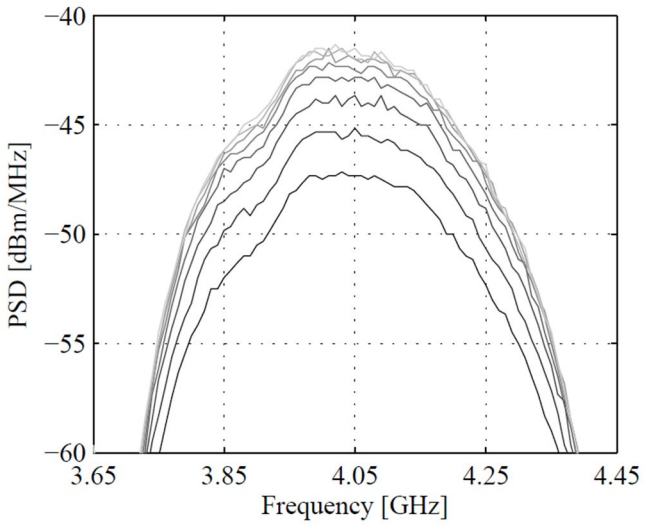

Figure 5-2: An example of linear-in-dB power adjustment.

ect conversion, a non-coherent and energy collection approach presented in [38]. The receiver includes the sensitivity of -67dBm with dynamic range of 27dB. The fully differential front-end design will be used, including a wideband LNA, Variable Gain Amplifier (VGA) and a Gilbert cell based multiplier [39] used for squaring operation which is the core of the non-coherent energy collection receiver together with integration. In the energy collection approach the received signal is simply squared and integrated over a certain time to detect the energy.

The architecture of the energy collection receiver is presented in Fig. 5-3. The received signal is filtered after the antenna to block all the off-band interferers. The bandwidth of the signal and the filt-

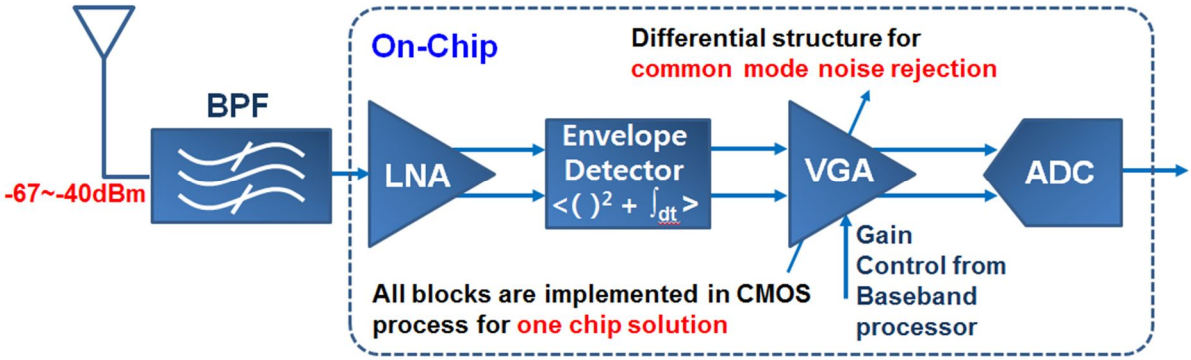

Figure 5-3: An example of energy collection receiver.

er is from 3.1GHz to 4.8GHz. After amplification, the filtered signal is squared in a Gilbert multiplier. The square signal is then integrated over a given time corresponding to the length of the transmitted pulse sequence. This non-coherent technique makes the receiver highly independent of the shape of the received waveform which further lowers the complexity and power consumption of the front-end receiver due to the fact that there is no need for complex frequency synthesis and template signal generation circuitries [38]. The UWB antenna and bandpass filter are off-chip components. The rest of the stages are integrated on a single chip.

As seen in Fig. 5-3, the gain of the VGA is controlled by the base-band signal processing circuitry. The digital Automatic Gain Control (AGC)-loop consists of the whole receiver from VGA to base-band signal processing. The output of the integrator, which is included in envelope detector, is monitored and based on the output value the gain is digitally adjusted to one of the pre-defined levels. The base-band signal processing takes also care of the post processing of the signal, including A/D conversion and bit decision.

The use of a VGA may be justified by the fact that the post processing of the signal is made digitally. The analog signal after the VGA is converted into digital by an A/D. The analog signal provided by the envelope detector and VGA, must be strong enough to exceed the threshold voltage level of the A/D. By controlling the gain of the receiver this is made possible. Also, the saturation and over-clipping of the analog circuits may be avoided by reducing gain in case of a strong signal.

Chapter VI

Summary & Conclusion

Ultra-WideBand (UWB) radio is suitable and optimal technology for wireless body area network (WBAN), due to its low power consumption characteristic as described in chapter I. The power consumption in most short-range wireless systems is dominated by the electronics and not the transmitted power. This is particularly true for UWB radios with a maximum transmit power allowed over the 3.1-10.6GHz band of only -2.5dBm. When the UWB band is divided in 500MHz channels, this transmit power reduces to -14.3dBm, or 37uW. Because power is dominated by the electronics, and with the amount of available bandwidth in the UWB band, it is not necessary to be spectrally efficient for low data rate applications. In fact, if the spectral efficiency may be sacrificed for reduced power consumption in the electronics, this can drastically reduce the overall system power consumption.

In chapter II, this thesis has investigated way to generate pulses optimally within the UWB band. An all-digital architecture is made practical by relaxing the frequency tolerance and spectral efficiency requirements, suitable for use with an energy detection receiver. Power is only consumed in sub-threshold leakage currents and dynamic switching losses, and no analog bias currents are required. The pulse spectrum is programmable in center frequency with a fixed pulse width, supporting a three-channel frequency plan from 3.1-4.8GHz. No RF oscillator is required by the transmitter; therefore, there is no startup time for generating pulses.

The low data rate transmitter communicates with an energy detection receiver using pulse position modulation (PPM). The form of PPM used is known to produce a spectrum with lines, even when modulated by purely random data. Therefore, some form of spectrum scrambling is required. BPSK scrambling is typically used to eliminate the tones; however, BPSK is costly to implement in an all-digital architecture. In this thesis, a spectrum scrambling technique termed delay-based BPSK (DB-BPSK) [23] is presented that can be implemented in the all-digital transmitter with minimal overhead as depicted in chapter III.

In conclusion, a novel technique to generate IR-UWB signal with the capability of variable channel selection was implemented in a standard 0.13-um CMOS technology. Its main feature is a fully digital architecture including a delay line and static logic gates without bias currents. The produced pulse occupies 3 channels form 3.1GHz to 4.8GHz, incorporating DAA requirement. The delay cell adjusts the center frequency and the 500MHz bandwidth for each channel, and it is digitally tuned. Intentional parasitic capacitor in the delay cell was formed to obtain the proper range of T_{delay} for linear

controllability. Self-referencing technique is used for unwanted-signal elimination. The combination of PPM and DB-BPSK phase scrambling, which is realized in the pulse generator, reduces magnitude of each prominent spectral line. Energy consumption of 48pJ/pulse makes it suitable for battery-operated devices employed in applications such as WBAN systems.

REFERENCES

1. Latré, B & Demeester, P 2011, 'A Survey on Wireless Body Area Networks', *Wireless Networks*, vol. 17, no. 1, pp. 1-18.

2. Chen, M & Leung, V 2011, 'Body Area Networks: A Survey', *Mobile Networks and Applications*, vol 16, no. 2, pp. 171-193.

3. Jovanov, E 2008, 'A Survey of Power Efficient Technologies for Wireless Body Area Networks', *Proc. of the 30th Annual International Conference of the IEEE Engineering in Medicine and Biology Society*, 20-24 August 2008, viewed 5 May 2010,

   http://ieeexplore.ieee.org/stamp/stamp.jsp?tp=&arnumber=4649992

4. Lee, J & Shen, C 2007, 'A Comparative Study of Wireless Protocols: Bluetooth, UWB, ZigBee, and Wi-Fi', *33rd Annual Conference of the IEEE, Industrial Electronics Society*, 5-8 November 2007, viewed 10 October 2010,

   http://ieeexplore.ieee.org/stamp/stamp.jsp?tp=&arnumber=4460126

5. Oppermann, I & Tonmazou, C 2004, 'UWB wireless sensor networks: UWSN-a practical example', *IEEE com, Mag.*, vol.42, no. 12, pp. 27-32.

6. Yuce, M & Ho, C 2008, 'Implementation of BAN based MMICs/WMTS medical bands for healthcare systems', IEEE Engineering in Medicine and Biology Society Conf.(EMBS'08), 20-25 August 2008, viewed 12 October 2010,

   http://ieeexplore.ieee.org/stamp/stamp.jsp?tp=&arnumber=4649940

7. Federal Communications Commission (FCC) 2002, *Revision of part 15 regarding ultra-wideband transmission systems*, First Report and Order, ET docket, FCC 02-48

8. MultiBand OFDM Physical Layer Proposal for IEEE 802.15 Task Group 3a, *MultiBand OFDM Alliance*, viewed 28 September 2010,

   www.wimedia.org

9. DS-UWB Physical Layer Submission to 802.15 Task Group 3a, *UWB Forum*, viewed 28 September 2010,

   www.uwbforum.org

10. Fontana, R & Barney, J 2003, 'Commercialization of an ultra wideband precision asset location system', *IEEE conference on Ultra Wideband Systems and Technologies*, viewed 28 October 2010,

http://ieeexplore.ieee.org/stamp/stamp.jsp?tp=&arnumber=1267866

11. Wireless Medium Access Control (MAC) and Physical Layer (PHY) Specifications for Low-Rate Wireless Personal Area Networks (LR-WPANs), *IEEE 802.15 Working Group*, viewed 11 November 2010,

http://profsite.um.ac.ir/~hyaghmae/ACN/WSNMAC1.pdf

12. Mishra, S, Brodersen, R, Brink, S & Mahadevappa, R 2007, 'Detect and Avoid: An Ultra-Wideband/WiMAX Coexistence Mechanism [Topics in Radio Communications]', *IEEE Communications Magazine*, vol. 45, no. 6, pp. 68-75.

13. Fernandes, J & Wentzloff, D 2010, 'Recent advances in IR-UWB transceivers: An overview', Proceedings of 2010 IEEE International Symposium on Circuits and Systems (ISCAS), 30 May 2010 – 2 June 2010, viewed 16 December 2010,

http://ieeexplore.ieee.org/stamp/stamp.jsp?tp=&arnumber=5537916

14. *Advertiser* 2005, 'Detect and Avoid Technology for Ultra Wideband Spectrum Usage', viewed 14 December 2010,

http://www.wisair.com/wp-content/DAA_WP.pdf

15. Leenaerts, D 2005, 'Ultra Wide Band Technology', *Philips Research Labs*, Eindhoven, the Netherlands, viewed 18 December 2010,

http://www.cmoset.com/uploads/Leenaerts.pdf

16. Scholtz, R & Win, M 1998, 'Impulse radio: how it works', *IEEE Communications Letters*, vol. 2, no. 2, pp. 36-38.

17. Ho, M, Taylor, L & Aiello, G 2001, 'UWB technology for wireless video networking', *Proc. IEEE Int. Conf. Consumer Electronics*, 19-21 June 2001, viewed 18 December 2010,

http://ieeexplore.ieee.org/stamp/stamp.jsp?tp=&arnumber=935194

18. Fontana, R, Ameti, A, Richley, E & Guy, D 2002, 'Recent advances in ultra wideband communications systems', *IEEE Conf. UWB Systems and Technologies*, pp. 129-133, viewed 18 December 2010,

http://ieeexplore.ieee.org/stamp/stamp.jsp?tp=&arnumber=1006333

19. Fleming, R, Kushner, C, Roberts, G & Nandiwada, U 2002, 'Rapid acquisition for ultra wideband localizers', *IEEE Conf. UWB Systems and Technologies*, pp. 245-249, viewed 18 December 2010,

    http://ieeexplore.ieee.org/stamp/stamp.jsp?tp=&arnumber=1006359

20. Proakis, J 1995, *Digital Communications, 3rd ed*., McGraw-Hill, New York.

21. Iida, S 2005, 'A 3.1 to 5 GHz CMOS DSSS UWB transceiver for WPANs', *IEEE International Solid-State Circuits Conference*, pp. 214-215, 594, viewed 15 December 2010,

    http://ieeexplore.ieee.org/stamp/stamp.jsp?tp=&arnumber=1493945

22. Azakkour, A, Regis, M, Pourchet, F & Alquie, G 2005, 'A new integrated monocycle generator and transmitter for ultra-wideband (UWB) communications', *IEEE Radio Frequency Integrated Circuit Symposium*, pp. 79-82, viewed 15 December 2010,

    http://ieeexplore.ieee.org/stamp/stamp.jsp?tp=&arnumber=1489592

23. Wentzloff, D & Chandrakasan, A 2007, 'A 47pJ/pulse 3.1 to 5GHz all-digital UWB transmitter in 90nm CMOS', *IEEE International Solid-State Circuits Conf.*, 11-15 February 2007, pp. 118-119, 591, viewed 14 December 2010,

    http://ieeexplore.ieee.org/stamp/stamp.jsp?tp=&arnumber=4242293

24. Bagga, S & Long, J 2004, 'A PPM Gaussian monocycle transmitter for ultra-wideband communications', *IEEE Conference on Ultra Wideband Systems and Technologies*, viewed 12 December 2010,

    http://ieeexplore.ieee.org/stamp/stamp.jsp?tp=&arnumber=1320950

25. Jeong, Y, Jung, S & Liu, J 2004, 'A CMOS impulse generator for UWB wireless communication systems', *International Symposium on Circuits and Systems*, viewed 12 December 2010,

    http://ieeexplore.ieee.org/stamp/stamp.jsp?tp=&arnumber=1328957

26. Marsden, K, Lee, H, Ha, D & Lee, H 2003, 'Low power CMOS re-programmable pulse generator for UWB systems', *IEEE Conference on Ultra Wideband Systems and Technologies*, viewed 12 December 2010,

    http://ieeexplore.ieee.org/stamp/stamp.jsp?tp=&arnumber=1267881

27. Kim, H, Park, D & Joo, Y 2004, 'All-digital low-power CMOS pulse generator for UWB system', *Electronics Letters*, vol. 40, no. 24, pp. 1534-1535.

28. Wentzloff, D & Chandrakasan, A 2006, 'Gaussian pulse Generator for subbanded ultra-wideband transmitters', *IEEE Transactions on Microwave Theory and Techn*iques, vol. 54, no. 4, pp. 1648-1655.

29. Zheng, Y, Arasu, A, Wong, K, The, Y, Suan, A, Tran, D, Yeah, W & Kwong, D 2008, 'A 0.18um CMOS 802.15.4a UWB Transceiver for Communication and Localization', *IEEE International Solid-State Circuits Conference*, 3-7 February 2008, pp. 118-119, 600, viewed 17 December 2010,

http://ieeexplore.ieee.org/stamp/stamp.jsp?tp=&arnumber=4523085

30. Mercier, P, & Chandrakasan, A 2008, 'A 19pJ/pulse UWB transmitter with dual capacitively-coupled digital power amplifiers', *IEEE Radio Frequency Integrated Circuit Symposium*, pp. 47-50, viewed 17 December 2010,

http://ieeexplore.ieee.org/stamp/stamp.jsp?tp=&arnumber=4561383

31. Sweeney, D 2002, 'Towards a Link Budget for Ultra WideBand (UWB) Systems', *Center for Wireless Telecommunication VA Tech*, Blacksburg, viewed 21 December 2010,

http://www.mprg.org/people/buehrer/ultra/protected/pdfs/UWB%20pathloss.pdf

32. Park, Y & Wentzloff, D 2008, 'All-Digital Synthesizable UWB Transmitter Architectures', *IEEE International Symposium on Ultra-Wideband*, Hannover, 10-12 September 2008, pp. 29-32, viewed 23 December 2010,

http://ieeexplore.ieee.org/stamp/stamp.jsp?tp=&arnumber=4653344

33. Rabaey, J & Chandrakasan, A 2003, *Digital Integrated Circuits: A Design Perspective, 2nd edition*, Prentice-Hall, pp. 458-459.

34. Park, Y & Wentzloff, D 2011, 'An All-Digital 12 pJ/Pulse IR-UWB Transmitter Synthesized From a Standard Cell Library', *IEEE J. Solid-Stat Circuits*, vol. 46, no. 5, May 2011, pp. 1747-1757.

35. Soldà, S & Neviani, A 2011, 'A 5Mb/s UWB-IR Transceiver Front-End for Wireless Sensor Networks in 0.13 um CMOS', *IEEE J. Solid-State Circuits*, vol. 46, no. 7, July 2011, pp. 1636-1647.

36. Crepaldi, M & Kenget, P 2010, 'An ultra-low-power interference-robust IR-UWB transceiver

chipset using self-synchronizing OOK modulation', *IEEE ISSCC Dig. Tech. Papers*, San Francisco, 7-12 February 2010, pp. 226-227, viewed 27 March 2011,

http://ieeexplore.ieee.org/stamp/stamp.jsp?tp=&arnumber=5433960

37. Mercier, P & Chandrakasan, A 2009, 'An energy-efficient all-digital UWB transmitter employing dual capacitively-coupled pulse-shaping drivers', *IEEE J. Solid-State Circuits*, vol. 44, no. 6, June 2009, pp. 1679-1688.

38. Rabbachin, A, Stoica, L, Tiuraniemi, S & Oppermann, I 2004, 'A Low Cost Low Power UWB Based Sensor Network', *International Workshop on Wireless Ad-Hoc Networks (IWWAN)*, 31 May – 3 June 2004, pp. 84-88, viewed 8 May 2011,

http://ieeexplore.ieee.org/stamp/stamp.jsp?tp=&arnumber=1525546

39. Gilbert, B 1968, 'A Precise Four-Quadrant Multiplier with Subnanosecond Response', IEEE J. Solid-State Circuits, vol. SC-3, no. 6, December 1968.

Acknowledgement

I owe the deepest gratitude to my supervisor, Prof. Franklin Bien. His encouragement, inspiration, guidance and support enabled me to develop an understanding of the research. I feel very lucky to be under the direction of Prof. Franklin Bien at UNIST.

I want to express my gratitude to Prof. Young Min Kim and Prof. Jin Kuk Kim for giving me advice about my research as a committee.

Thanks to Ph.D. Jin Doo Jung (at ETRI) for giving me so much information to build up system specifications.

I would like to thank my lab members, BICDL people. They gave me a valuable advice and encouragement.

Lastly, I really appreciate my parents giving me the most valuable affection to study so far.